



HAL
open science

On the promotional effect of Pd on the propene-assisted decomposition of NO on chlorinated Ce_{0.68} Zr_{0.32} O₂

Cyril Thomas, Olivier Gorce, Céline Fontaine, Jean-Marc Krafft, Françoise Villain, Gérald Djéga-Mariadassou

► To cite this version:

Cyril Thomas, Olivier Gorce, Céline Fontaine, Jean-Marc Krafft, Françoise Villain, et al.. On the promotional effect of Pd on the propene-assisted decomposition of NO on chlorinated Ce_{0.68} Zr_{0.32} O₂. Applied Catalysis B: Environmental, 2006, 63, pp.201-214. hal-00181040

HAL Id: hal-00181040

<https://hal.science/hal-00181040>

Submitted on 23 Oct 2007

HAL is a multi-disciplinary open access archive for the deposit and dissemination of scientific research documents, whether they are published or not. The documents may come from teaching and research institutions in France or abroad, or from public or private research centers.

L'archive ouverte pluridisciplinaire **HAL**, est destinée au dépôt et à la diffusion de documents scientifiques de niveau recherche, publiés ou non, émanant des établissements d'enseignement et de recherche français ou étrangers, des laboratoires publics ou privés.

1
2 **On the promotional effect of Pd**
3 **on the propene-assisted decomposition of NO**
4 **on chlorinated Ce_{0.68}Zr_{0.32}O₂**

5
6 Cyril Thomas*, Olivier Gorce¹, Céline Fontaine, Jean-Marc Krafft, Françoise Villain² and
7 Gérard Djéga-Mariadassou

8
9 Laboratoire de Réactivité de Surface, UMR CNRS 7609, Université Pierre et Marie Curie, 4
10 Place Jussieu, Case 178, 75252 Paris cedex 05, France

11 ¹Present address: Renault sas, Centre Technique de Lardy, 1 allée Cornuel, 91510 Lardy,
12 France

13 ²Laboratoire de Chimie Inorganique et Matériaux Moléculaires, UMR CNRS 7071,
14 Université Pierre et Marie Curie, 4 Place Jussieu, 75252 Paris cedex 05, France

15
16 **Running title:** C₃H₆-assisted decomposition of NO on PdO_x/Ce_{0.68}Zr_{0.32}O₂ catalysts

17
18 * To whom correspondence should be addressed:

19 Dr. Cyril Thomas

20 Laboratoire de Réactivité de Surface, UMR CNRS 7609, case 178, Université P. et M. Curie,
21 4 Place Jussieu 75252 Paris Cedex 05, France

22 e-mail: cthomas@ccr.jussieu.fr

23 Tel: + 33 1 44 27 36 30

24 Fax: + 33 1 44 27 60 33

1 **Abstract:**

2 The Selective Catalytic Reduction (SCR) of NO_x assisted by propene is investigated
3 on Pd/Ce_{0.68}Zr_{0.32}O₂ catalysts (Pd/CZ), and is compared, under identical experimental
4 conditions, with that found on a Pd/SiO₂ reference catalyst. Physico-chemical characterisation
5 of the studied catalysts along with their catalytic properties indicate that Pd is not fully
6 reduced to metallic Pd for the Pd/CZ catalysts. This study shows that the incorporation of Pd
7 to CZ greatly promotes the reduction of NO in the presence of C₃H₆. These catalysts display
8 very stable deNO_x activity even in the presence of 1.7% water, the addition of which induces
9 a reversible deactivation of about 10%. The much higher N₂ selectivity obtained on Pd/CZ
10 suggests that the lean deNO_x mechanism occurring on these catalysts is different from that
11 occurring on Pd⁰/SiO₂. A detailed mechanism is proposed for which CZ achieves both NO
12 oxidation to NO₂ and NO decomposition to N₂, whereas PdO_x activates C₃H₆ via ad-NO₂
13 species, intermediately producing R-NO_x compounds that further decompose to NO and
14 C_xH_yO_z. The role of the latter oxygenates is to reduce CZ to provide the catalytic sites
15 responsible for NO decomposition. The proposed C₃H₆-assisted NO decomposition
16 mechanism stresses the key role of NO₂, R-NO_x and C_xH_yO_z as intermediates of the SCR of
17 NO_x by hydrocarbons.

18

19

20 **Key Words:** CO-FTIR, XANES, Lean deNO_x, Mechanism, C₃H₆, Pd catalysts, Ceria-
21 Zirconia, TPD of NO_x

22

1 **1. Introduction**

2 A tremendous number of investigations have been made within the past decades to
3 develop catalysts capable of decreasing the emissions of air pollutants such as carbon
4 monoxide (CO), hydrocarbons (HC) and nitrogen oxides (NO_x) from automotive gas exhausts
5 [1-6]. The development of improved catalysts to meet the ever more stringent emissions
6 standards is, however, still of key importance. To achieve this goal, the most promising means
7 would obviously be to find a catalytic system that could directly decompose NO over a wide
8 range of temperatures as pointed out by Pârvulescu et al. in a rather recent review [4].
9 Although a large number of catalysts have already been tested, no such system has as yet been
10 found.

11 Three-Way Catalysts (TWC) were among the first possibilities investigated for lean
12 NO_x abatement in car exhausts. These catalysts, which typically operate with an air-to-fuel
13 ratio (A/F) close to the stoichiometry [1,5-7], are generally made up of a quite complicated
14 combination of noble metals supported on an oxide carrier. These noble metals have shown to
15 dissociate readily NO when present in their fully reduced state [1,2,4,8-10].

16 In addition to the ever more restricting limitations on carbon monoxide and nitrogen
17 oxides, new regulations have appeared concerning the emission of carbon dioxide which is
18 well known to be one of the greenhouse gases responsible for global warming. From this
19 point of view, diesel engines, which operate typically under a lean mixture (air-to-fuel ratio
20 (A/F) greater than unity), is among the solutions that must be considered to meet the CO₂
21 emission requirements. Indeed, such burning conditions lead to a lowering of fuel
22 consumption and consequently to a decrease of the CO₂ emissions. Although these lean
23 conditions have solved essentially the carbon monoxide and unburned hydrocarbon emission
24 problems, they have made the classic TWC ineffective in removing nitrogen oxides from lean
25 automotive gas exhausts.

1 The catalytic solution using a traditional TWC associated with a storage component
2 (barium carbonate: BaCO₃) [11] which has been adopted for lean gasoline engines has still to
3 be adapted for diesel cars which, as yet, have no suitable catalytic solution. A more attractive
4 alternative would be to develop a specific catalyst capable of reducing nitrogen oxide
5 emissions under lean conditions.

6 Among all the different formulations evaluated, to date, zeolite-based catalysts are
7 probably those which have been studied most [3,4]. This might be due to the promising
8 findings of Iwamoto et al. [12,13] and Lee and Armor [14] who showed that Cu-exchanged
9 ZSM5 is able to decompose nitrogen monoxide at RT. This decomposition process is,
10 however, self-inhibiting since as soon as nitrogen monoxide is decomposed on the catalytic
11 sites (copper ions) they are poisoned by the oxygen left from nitrogen monoxide
12 decomposition and, thus, the reaction stops. It is important to notice the striking similarity
13 with model TWC reported in the case of stoichiometric mixture by Djéga-Mariadassou and
14 co-workers [7,15,16]. These authors demonstrated the competition between the CO oxidation
15 reaction and the assisted decomposition of NO by CO. In lean exhausts, carbon monoxide
16 cannot be further used to assist the decomposition of nitrogen monoxide [16]. Consequently,
17 other reductants such as hydrocarbons must be used to assist the decomposition of nitrogen
18 monoxide. In the case of model exhausts, it has been shown by Matsumoto et al. [17] that
19 alkenes, and more particularly propene, are the most efficient reductants to assist the nitrogen
20 monoxide reduction. Alkenes are, however, also known as coke precursors for acidic catalysts
21 which accounts for the dramatic deactivation of zeolite-based catalysts when propene is
22 present in the lean mixture [18]. In addition to this coking phenomenon, zeolite-based
23 catalysts are rather sensitive to water, and deactivation was also reported due to their low
24 hydrothermal resistance [4]. These drawbacks have led researchers to focus on oxides-
25 supported Platinum Group Metals (PGMs) catalysts. Due to their intrinsic higher activity [19-

21], supported Pt catalysts have been the subject of the greatest number of studies [9,22-33]. These are followed by supported Rh [10,19-21,33] and Pd [19-21,33,34] catalysts. Although these catalysts exhibit significant lean deNO_x activity with C₃H₆ as reductant and quite reasonable stability, they have a rather narrow temperature operating window [19] and fairly poor selectivity to N₂ [9,30,34,35]. N₂O, which is well known as a component of the greenhouse effect [36], is, indeed, formed in substantial amounts. High selectivity to N₂ has, however, been reported for Rh/Al₂O₃ catalysts [10,19,33]. Alumina-supported Rh catalysts usually operate at much higher temperatures than either supported Pt or Pd catalysts. This peculiarity led Obuchi et al. to the conclusion that this high selectivity to N₂ was attributable to an additional catalytic effect of the alumina support [33]. The influence of the nature of the support was also investigated [19,20,30]. These studies, however, did not report on PGMs supported on ceria-zirconia (CZ) until recently for Rh/CZ [37] or Pt catalysts supported on CZ-Al₂O₃ [31] and pure CZ [32]. Finally, CZ showed only very moderate lean deNO_x activity in the presence of C₃H₆ [38].

The aim of this work is to investigate the influence of Pd addition to a chlorinated ceria-zirconia support on lean deNO_x with C₃H₆ as reductant. To our knowledge, such catalysts have not been investigated for this particular reaction. They have, however, been widely studied in the fields of TWC [39-43], CH₄ total oxidation [44,45] and hydrocarbon reforming [46]. For comparison, the performances of a Pd/SiO₂ catalyst are also reported. Pd/CZ catalysts show enhanced lean deNO_x activity and much higher N₂ selectivity compared to Pd/SiO₂. This suggests the involvement of distinct lean deNO_x reaction mechanisms within these two catalytic systems. Based on transient and steady-state experiments, a mechanism of the lean deNO_x is proposed for the Pd/CZ catalysts.

24

25

1 **2. Experimental**

2

3 *2.1. Catalyst synthesis*

4 *2.1.1. Ceria-zirconia ($Ce_{0.68}Zr_{0.32}O_2$: CZ)*

5 The CZ solid solution was provided by Rhodia. The CZ was added to chloridric acid
6 solution (pH 1.9) prepared by adding HCl to distilled water. After ageing for 2 hours under
7 vigorous stirring, CZ was filtered and washed with distilled water before being dried in air at
8 120°C for 3 hours.

9

10 *2.1.2. Pd/CZ*

11 Two ceria-zirconia-supported Pd catalysts (0.54 and 0.89 wt% Pd) were prepared by
12 incipient wetness impregnation of the chlorinated support by an aqueous solution of PdCl₂,
13 3H₂O (Johnson Matthey). After impregnation, the catalysts were aged for 2 hours and dried in
14 air at 120°C for three hours.

15

16 *2.1.3. Pd/SiO₂*

17 For comparison with Pd/CZ catalysts, a silica (Degussa, Aerosil 50)-supported
18 palladium catalyst (0.93 wt% Pd) was prepared by incipient wetness impregnation of the
19 support by an aqueous solution of PdCl₂, 3 H₂O (Johnson Matthey). After impregnation, the
20 catalyst was aged for 2 hours and dried in air at 120°C for three hours.

21

22 *2.2. Catalyst characterization*

23 Metal and chlorine contents were determined by chemical analyses (CNRS –
24 Vernaison). The chlorine content was about 1 wt% for the CZ-based catalysts before and after
25 reaction.

1 The specific surface areas were determined by physisorption of N₂ at 77K using a
2 Quantasorb Jr. dynamic system equipped with a thermal conductivity detector (TCD). The
3 specific surface areas were calculated using the BET method. For CZ-supported catalysts, the
4 specific surface areas were about 100 m² g⁻¹ before and after testing, whereas that of Pd/SiO₂
5 was about 50 m² g⁻¹.

7 *2.2.1 Determination of the percentage of exposed zero-valent Pd atom (PEM⁰)*

8 With the well-known reducibility of the CZ support [47], the determination of the
9 percentage of exposed zero-valent Pd atom was done by means of propene hydrogenation
10 [48].

11 Prior to propene hydrogenation, the catalyst sample (30-60 mg deposited on sintered
12 glass of a pyrex reactor) was heated in flowing H₂ (100 mL_{NTP} min⁻¹) at atmospheric pressure
13 with a heating rate of 3°C min⁻¹ up to 300°C and was kept at this temperature for 2h. After
14 cooling to -78°C under H₂, the reaction was started. The partial pressure of propene was 51.8
15 torr, and the total flow rate was 107 mL_{NTP} min⁻¹ with H₂ as balance.

16 The composition of the effluents was analyzed by means of an on-line gas
17 chromatograph (Hewlett Packard 5890, FID) equipped with a CP-Al₂O₃/KCl (Chrompack,
18 50 m long, 0.32 mm inner diameter, 5 µm film thickness) capillary column. The only detected
19 product was propane.

20 From the initial reaction rates obtained, the numbers of exposed zero-valent Pd atoms
21 were calculated according to a turnover rate of 0.40 s⁻¹ for the propene hydrogenation reaction
22 at -78°C [48].

1 2.2.2. *Temperature-Programmed Reduction*

2 Temperature-Programmed Reduction (TPR) experiments were performed in a
3 conventional system equipped with a thermal conductivity detector. After calcination at
4 500°C for 2h, the reduction was carried out in a flow of H₂ (5%) in Ar (25 mL min⁻¹) using a
5 heating rate of 5°C min⁻¹. Typically, the reduction was carried out up to 700°C and then the
6 sample (0.02-0.05 g) was kept at this temperature for 15 min. H₂O evolving in the course of
7 the TPR experiments was trapped by a 5A molecular sieve. The amount of H₂ uptake in the
8 TPR was estimated from integrated peak areas.

9

10 2.2.3. *X-Ray diffraction*

11 X-Ray diffraction (XRD) patterns of CZ, SiO₂, Pd(0.93)/SiO₂ and Pd/CZ were
12 obtained on a SIEMENS D500 diffractometer with a Cu K_α monochromatized radiation.

13

14 2.2.4. *X-ray absorption near edge spectroscopy (XANES)*

15 X-Ray absorption measurements were carried out using synchrotron radiation of the
16 XAS13 station at LURE (Orsay, France) on line D42 (May 3-4, 2001). Fluorescence yield
17 spectra of Pd(0.54)/CZ were recorded at RT using a Ge solid detector (Eurisyss, 7 elements)
18 combined with a multichannel analyser to select the Pd K_α fluorescence, whereas those of the
19 reference compounds (Pd foils, 20 μm thick, PdO (> 99% pure, Lancaster)) were collected in
20 the transmission mode. The incident beam was monochromatized using a Ge (400) double
21 monochromator. XANES spectra were collected at the Pd K edge with a sampling step of 2.0
22 eV/point from 24300 to 24500 eV and an integration time of 10s and 2s in fluorescence and
23 transmission modes, respectively. The energy was calibrated using the Pd foil. XANES
24 spectra were obtained from Pd(0.54)/CZ either after oxidation or reduction treatments under
25 flowing air or H₂ (100 mL_{NTP} min⁻¹) for 2h at 500°C. To avoid the exposure of the reduced

1 sample to O₂, the catalyst was then transferred into a UV cell (Suprasil quartz, 5 cm long, 1 cm
2 wide and 1 cm high) that was finally sealed under vacuum (5×10^{-5} torr). In the case of the
3 oxidized sample, we checked that the high purity silica glass did not interfere with incident
4 and fluorescent beams. Superimposed spectra were, indeed, obtained with this sample located
5 either into the UV cell or between Kapton tapes. The cell was set to 45° with respect to the
6 incident RX beam and the fluorescence detector. The extraction of the data was done with
7 Michalowicz's software package [49,50].

8

9 *2.2.5. Fourier transform infra-red spectroscopy*

10 Fourier transform infra-red (FTIR) spectra of adsorbed CO on CZ and Pd(0.89)/CZ
11 were collected on a Bruker Vector 22 FTIR spectrometer equipped with a liquid N₂-cooled
12 MCT detector and a data acquisition station. 256 scans were averaged with a spectral
13 resolution of 2 cm⁻¹.

14 The samples were pressed into self-supporting wafers of 6-11 mg cm⁻². The wafers
15 were loaded in a moveable glass sample holder, equipped on top with an iron magnet, inserted
16 in a conventional pyrex-glass cell (CaF₂ windows) connected to a vacuum system. The iron
17 magnet allowed the transfer of the catalyst sample from the oven-heated region to the infrared
18 light beam.

19 Prior to adsorption of CO, the catalysts were submitted to a dynamic (50 cm³ min⁻¹)
20 reducing pretreatment (5% H₂ in Ar, Air Liquide, 99.999%) at 500°C for 2 h at atmospheric
21 pressure. The catalyst samples were then evacuated (10⁻⁶ mbar) at 500°C for 60 min before
22 the temperature was decreased to RT under dynamic vacuum.

23 CO (Air Liquide, 99.999%), trapped at 77 K, was adsorbed at RT at equilibrated
24 pressures of 0.9 and 18 torr.

1 The spectrum of the pretreated catalyst was used as reference and subtracted from the
2 spectra of the catalyst exposed to CO.

3

4 *2.3. Catalytic runs*

5 Prior to catalytic runs, the samples were calcined in situ in dry air at 500°C
6 (4°C.min⁻¹) for 2 hours with a flow rate of 500 mL_{NTP} min⁻¹ per gram of catalyst.

7 Steady-state, Temperature-Programmed Desorption (TPD) and Temperature-
8 Programmed Surface Reaction (TPSR) experiments and were carried out. After being
9 contacted with the appropriate gas mixture at RT, temperature transient experiments were
10 carried out from RT to 500°C with a heating rate of 10°C min⁻¹. Before the TPD experiments,
11 the catalyst samples were flushed in N₂ to remove RT physisorbed species from the
12 adsorption mixture.

13 The experiments were carried out in a U-type quartz reactor. The sample (0.2 g unless
14 otherwise specified) was held between plugs of quartz wool, and the temperature was
15 controlled through a WEST 4000 temperature controller using a K type thermocouple.
16 Reactant gases were fed from independent mass flow controllers (Brooks 5850E). The total
17 flow was 250 mL_{NTP} min⁻¹ to which corresponds a HSV (Hour Space Velocity) of
18 112,500 h⁻¹.

19 Catalytic experiments were carried out with C₃H₆ as reductant. Typically, the
20 composition of the C₃H₆-NO-O₂ reacting mixture was: 1900 ppm C₃H₆, 340 ppm NO and 8%
21 O₂ in N₂. The reactants, diluted in N₂, were fed from independent gas cylinders (Air Liquide).

22 The reactor outflow was continuously analysed using the combination of four different
23 detectors. An Eco Physics CLD 700 AL chemiluminescence NO_x analyser (for NO and total
24 NO_x (*i.e.* NO + NO₂)) allowed the simultaneous detection of both NO and NO_x. Two Ultramat
25 6 IR analysers were used to monitor N₂O, CO and CO₂. A FID detector (Fidamat 5A) was

1 used to follow the concentration of hydrocarbons. We checked that, under our experimental
 2 conditions, CO and CO₂ had a negligible response on the N₂O IR analyser, whereas that of
 3 C₃H₆ was significant. C₃H₆ contribution to the N₂O signal was taken into account to calculate
 4 the "true" N₂O concentration ([N₂O]) as follows (Eq. 1):

$$5 \quad [N_2O] = [N_2O]_{\text{meas.}} - \frac{[N_2O]^0 \times [C_3H_6]_{\text{meas.}}}{[C_3H_6]_{\text{inlet}}} \quad (1)$$

6 where [N₂O]⁰, [C₃H₆]_{inlet}, [C₃H₆]_{meas.} and [N₂O]_{meas.} are: the concentrations of N₂O due to the
 7 contribution of the inlet concentration of C₃H₆, the inlet concentration of C₃H₆, C₃H₆ and N₂O
 8 concentrations measured in the course of the reaction, respectively. As N₂ was used as
 9 balance, the conversion of NO_x to N₂ was calculated assuming 100% nitrogen mass balance
 10 (Eq. 2):

$$11 \quad \text{Conversion of NO}_x \text{ to N}_2 \text{ (\%)} = \frac{[NO_x]_{\text{inlet}} - ([NO_x]_{\text{outlet}} + 2 \times [N_2O])}{[NO_x]_{\text{inlet}}} \quad (2)$$

12 where [NO_x]_{inlet} and [NO_x]_{outlet} are the concentrations of NO_x at the inlet and at the outlet of
 13 the reactor, respectively.

14 In one experiment, over Ce_{0.68}Zr_{0.32}O₂, propene was substituted by 1-propanol (Merck,
 15 spectroscopic grade) with a concentration of 2200 ppm by means of a saturator.

16

17 **3. Results**

18

19 *3.1. Catalyst characterization*

20 *3.1.1. Determination of the percentage of exposed zero-valent metal atoms (PEM⁰)*

21 Table 1 lists the percentage of exposed zero-valent palladium atoms of the CZ-
 22 supported Pd catalysts and Pd(0.93)/SiO₂. The percentage of exposed zero-valent Pd atoms is
 23 about 17 and 22% for Pd/CZ and Pd(0.93)/SiO₂, respectively.

1 3.1.2. TPR results

2 Fig. 1 shows the TPR profiles of the calcined catalysts. For Pd(0.93)/SiO₂, the trace of
3 which is magnified by a factor of 4 for the sake of clarity, a reduction peak is observed at
4 about 50°C.

5 For the CZ sample, the trace of which is magnified by a factor of 3, a broad reduction
6 peak starting around 400°C and ranging to a maximum at 530°C is observed. This reduction
7 temperature region corresponds well with that reported for various ceria-zirconia materials
8 [51-55].

9 The presence of noble metal on CZ modifies substantially the features of the TPD
10 profiles. Indeed, the reduction peak revealed over the CZ sample vanishes, while a strong
11 signal appears at temperatures below 200°C depending on the catalyst sample. It is observed
12 that the reduction peak shifts to lower temperature with increasing Pd content. Luo and Zheng
13 [56] reported a similar feature despite the fact that their TPR traces were substantially
14 different from ours.

15 As it is well established that the incorporation of noble metals increases the
16 reducibility of the ceria-related materials [47,51,52,56,57], quantitative analysis of the TPR
17 traces is not discussed. Overall, the amount of H₂ consumed in the course of the TPR was
18 close to 0.5 10⁻³ mol g⁻¹ for all samples. This value agrees well with those listed by Luo and
19 Zheng for Ce_{0.5}Zr_{0.5}O₂-supported Pd catalysts [56].

20 Finally, the comparison of the TPR traces of Pd(0.93)/SiO₂ and Pd(0.89)/CZ clearly
21 shows that the Pd species interact to a greater extent with CZ than with SiO₂. The reduction
22 peak of these Pd species supported on CZ is, indeed, shifted to higher temperature compared
23 with that of Pd(0.93)/SiO₂.

24

25

1 3.1.3. XRD

2 XRD patterns of the calcined SiO₂, Pd(0.93)/SiO₂ and CZ samples are shown in Fig. 2.
3 After calcination of Pd(0.93)/SiO₂, a diffraction peak is observed at about 33.8° which
4 corresponds to PdO (101 plane). Two very weak peaks at about 41.9 and 54.8° can also be
5 assigned to PdO. As shown in Fig. 2, the diffraction pattern of CZ exhibits 4 peaks at about
6 29, 33.8, 48.3 and 57.2°. Owing to the weak intensity of the PdO peaks and the overlapping
7 with CZ support, the presence of PdO on the CZ-supported catalysts could not be established
8 through XRD.

9

10 3.1.4. XANES measurements

11 XANES spectra of the Pd(0.54) catalyst after calcination or reduction are shown in
12 Fig. 3. The shape of the XANES spectra of the Pd(0.54)/CZ sample either calcined (----) or
13 reduced (—) corresponds fairly well to that of the PdO (▲) and Pd metal (Δ) references (Fig.
14 3), respectively. This result markedly differs from that of the reduced Rh/CZ catalyst, which
15 showed a XANES spectrum different from both Rh foil and Rh₂O₃ references [58].

16

17 3.1.5. IR

18 The CO-FTIR technique was used to probe the nature of the metal species [59]
19 supported on CZ.

20 The FTIR spectra of adsorbed CO under equilibrated pressures of 0.9 and 18 torr of
21 CO are shown in Fig. 4 for CZ and Pd(0.89)/CZ. It is worthwhile noting the fairly low
22 intensity of the CO absorption bands. This is why the CO-FTIR of the Pd(0.54)/CZ catalyst
23 was not investigated.

24 Over CZ (Fig. 4a), two CO absorption bands are observed at 1575 and 2167 cm⁻¹. The
25 band at 1575 cm⁻¹ can be assigned to the formation of carbonates [60]. This band appears as

1 soon as the equilibrated pressure of CO is 0.9 torr, whereas the band at 2167 cm^{-1} is observed
2 only at a pressure of 18 torr. This latter band has been attributed to the weak interaction of CO
3 with Ce surface sites [61-64].

4 The FTIR spectra of adsorbed CO on Pd(0.89)/CZ (Fig. 4b) differ markedly from
5 those of CZ. The formation of carbonate is not observed, and a rather broad absorption band
6 from 1850 to 2090 cm^{-1} is revealed, with two maxima at 1950 and 2083 cm^{-1} . The band at
7 1950 cm^{-1} , also found in a previous work of Badri et al. on a chlorinated Pd/CeO₂ sample
8 [61], can be assigned to bridged CO species bonded to zero-valent Pd atoms (Pd⁰₂CO)
9 [43,65,66]. In contrast, the band with the maximum at 2083 cm^{-1} corresponds to CO species
10 singly bonded to Pd⁰ atoms [43,59,61,63,65]. CO coordinated to Ce^{Z+} centers, acting as Lewis
11 acid sites, gives rise to an absorption band at 2175 cm^{-1} , as already reported by Badri et al.
12 [61].

13

14 3.1.6. NO oxidation

15 As reported earlier [38 and references therein], the oxidation of NO to NO₂ is
16 suspected to be an essential step of the deNO_x process. This reaction was, thus, investigated
17 over CZ and Pd(0.54)/CZ under steady-state conditions. As shown in Fig. 5, NO oxidation is
18 the greatest at 400°C. At higher temperatures, the conversion of NO decreases due to
19 thermodynamic limitations. It is important to note that the addition of Pd does not promote
20 NO oxidation, and this reaction is only catalysed by the CZ support.

21

22 3.1.7. Adsorption of NO-O₂ – TPD in N₂

23 Fig. 6 shows the NO_x TPD profiles in N₂ of samples contacted with NO-O₂ (340 ppm-
24 8%). The addition of Pd to CZ does not affect the TPD profiles to a large extent. In both
25 cases, two NO peaks are observed at about 100 and 420°C, and a broad NO₂ desorption

1 profile is seen from 50 to 450°C. This NO₂ feature exhibits two maxima at low and high
2 temperatures. The high temperature maximum is close to 350°C and is not affected by the
3 introduction of Pd. In contrast, the low temperature maximum shifts from 116 to 136°C when
4 Pd is added to CZ (Fig. 6c). For both samples, the quantities of adsorbed and desorbed NO_x
5 closely match (Table 2). Table 2 shows that the amount of adsorbed NO_x fluctuates to some
6 extent. This was related to slightly different times of exposure and not to differences in the
7 starting conditions of the samples. In agreement with previous work [67], PdO/SiO₂ did not
8 chemisorb NO_x. Consequently, the TPD in C₃H₆-O₂ after NO_x chemisorption was not
9 performed.

10

11 *3.1.8. Adsorption of NO-O₂ – TPD in C₃H₆-O₂*

12 After exposure of the samples to a NO-O₂ mixture, the TPD profiles obtained in C₃H₆-
13 O₂ are shown in Fig. 7 for CZ and Pd(0.89)/CZ. Before TPD, the samples were flushed by N₂
14 to remove physisorbed NO_x and then contacted with the desorption gas mixture (C₃H₆-O₂) for
15 a few minutes at RT. For both samples, a C₃H₆ desorption profile is observed at low
16 temperature. It is worth mentioning that in the case of the oxidation of C₃H₆ by O₂ without
17 pre-adsorption of NO_x (not shown), a similar desorption feature was observed. This low
18 temperature desorption feature is, thus, attributed to propene species chemisorbed on catalytic
19 sites different from those occupied by adsorbed NO_x species. For both catalysts, HC
20 consumption starts at 80°C and a more drastic HC consumption is observed at about 110°C. It
21 is worthwhile mentioning that the HC consumption profile is slightly different for
22 Pd(0.89)/CZ compared with that of CZ. At temperatures higher than 150°C, the HC
23 concentration reaches its input concentration for CZ (Fig. 7a). This phenomenon, however, is
24 not observed for Pd(0.89)/CZ (Fig. 7b). The first column of Table 3 shows that the light-off

1 temperature of C_3H_6 in the course of the TPD in $C_3H_6-O_2$ decreases drastically with the
2 addition of Pd.

3 Considering desorption of the N_tO_x (NO , NO_2 and N_2O) species, rather complicated
4 profiles are observed (Fig. 7). A detailed description of the traces seen for CZ is reported in a
5 recent article [38]. The amounts of adsorbed and desorbed N_tO_x species are listed in Table 2.
6 For both catalysts, a comparison of the desorbed quantities (Table 2) and profiles of N_tO_x
7 species of the two TPD experiments either in N_2 (Fig. 6) or in $C_3H_6-O_2$ (Fig. 7) after exposure
8 of the samples to $NO-O_2$ shows striking differences. First, NO becomes the major N_tO_x
9 species of the TPD in $C_3H_6-O_2$. In contrast, NO_2 is the major species of the TPD in N_2 .
10 Second, the global amount of desorbed N_tO_x species, taking into account that N_2O originates
11 from the recombination of two NO_x molecules, is always lower than that adsorbed for the
12 TPD in $C_3H_6-O_2$. On the other hand, adsorbed and desorbed NO_x quantities agree well for the
13 TPD in N_2 . These results suggest that part of the adsorbed NO_x is reduced to N_2 in the
14 presence of C_3H_6 in the desorption mixture. Finally, the N_tO_x TPD profiles (Fig. 7) suggest
15 that part of the adsorbed NO_x species reacted with C_3H_6 in the low temperature region (50-
16 $115^\circ C$). For N_tO_x species, the NO_x desorption feature is clearly truncated in this low
17 temperature region compared to that of the TPD in N_2 (Fig. 6). As already discussed [38],
18 these concomitant consumptions suggest the interaction of adsorbed NO_x species ($ad-NO_x$)
19 with propene and the formation of mixed compounds ($R-NO_x$) stored on the catalytic
20 material. For Pd(0.89)/CZ, it is worth adding that a stabilised HC consumption occurs up to
21 higher temperatures, ca. $150^\circ C$, compared with that observed on CZ (Fig. 7). Overall, the
22 broad N_tO_x desorption features observed at low temperatures ($100-200^\circ C$) over CZ become
23 thinner over Pd(0.89)/CZ, whereas those at high temperatures ($220-400^\circ C$) are clearly shifted
24 to lower temperatures ($200-300^\circ C$) with the incorporation of Pd. In addition, the amount of

1 NO₂ desorbed at temperatures higher than 200°C is much lower over Pd(0.89)/CZ than over
2 CZ. That of N₂O is, however, greater.

3

4 *3.1.9. C₃H₆ oxidation by O₂*

5 Fig. 8 shows that the C₃H₆ oxidation profiles are obviously different depending on the
6 nature of the catalyst support.

7 On Pd(0.89)/CZ, C₃H₆ oxidation is rather similar to that observed after adsorption of
8 NO-O₂ (Fig. 7b) with comparable light-off temperature (Table 3). On such a catalyst,
9 however, the consumption of C₃H₆ in the C₃H₆-O₂ reaction starts at a higher temperature and
10 is more pronounced before 250°C than after adsorption of NO-O₂. In contrast, C₃H₆ oxidation
11 proceeds much more steeply in a much narrower range of temperature (from 195 to 260°C) on
12 Pd(0.93)/SiO₂ than on Pd(0.89)/CZ (Fig. 8). In addition, C₃H₆ does not chemisorb at RT on
13 Pd(0.93)/SiO₂, as is the case of Pd(0.89)/CZ that shows a low temperature C₃H₆ desorption
14 feature. For Pd(0.93)/SiO₂, it is worthwhile noting that the experiment reported on Fig. 8 was
15 carried out after a previous C₃H₆-NO-O₂ Temperature-Programmed Surface Reaction (TPSR).
16 It will be shown later (please refer to part 3.1.10.) that for Pd(0.93)/SiO₂ such an experimental
17 sequence does significantly influence the light-off temperature of C₃H₆, whereas it has no
18 impact on CZ-supported catalysts.

19 Table 3 shows that the C₃H₆ light-off temperature for the C₃H₆-O₂ reaction is the
20 lowest for Pd(0.93)/SiO₂ and the highest for CZ. Finally, Pd promotes significantly C₃H₆
21 oxidation for the CZ-based catalysts.

22

23 *3.1.10. C₃H₆-NO-O₂ TPSR experiment*

24 TPSR of the complete reacting mixture was performed after exposure of Pd(0.89)/CZ
25 to the reacting mixture at RT (Fig. 9). The features observed are comparable to those seen for

1 the TPD in $C_3H_6-O_2$ after adsorption of $NO-O_2$ (Fig. 7b). NO desorption is the major N_tO_x
2 species with a two peak profile (100 and 220°C). The formation of NO_2 and N_2O are,
3 however, more limited than those obtained for the TPD experiment in $C_3H_6-O_2$ (Fig. 7). C_3H_6
4 and NO_x consumptions detected in the low temperature region in the case of the TPD
5 experiment in $C_3H_6-O_2$ are no longer observed. C_3H_6 is moderately consumed from 100 to
6 200°C and at higher temperatures the oxidation of C_3H_6 accelerates. More interesting is that
7 the NO_x profile shows a decrease of the NO_x concentration at 297°C corresponding to 50% of
8 the NO_x inlet concentration. At this temperature, the conversion of C_3H_6 is 79%. At higher
9 temperatures, the NO_x concentration reaches back its inlet concentration, and NO is oxidized
10 to NO_2 when full conversion of C_3H_6 is achieved at about 400°C.

11 Compared with the TPSR profiles found on CZ (Fig. 12 of [38]), the desorption peak
12 of NO reported in this experiment at about 300°C is no longer observed in the course of the
13 TPSR on $Pd(0.89)/CZ$, as a NO_x deficit occurs in this temperature range (Fig. 9).

14 The TPSR profiles of $Pd(0.93)/SiO_2$ (not shown) are less complicated than those of
15 $Pd(0.89)/CZ$. The most interesting peculiarity is that if the temperature is decreased from
16 500°C to RT (reverse TPSR) after the first TPSR experiment, the C_3H_6 light-off temperature
17 and the selectivity to N_2 are modified significantly. The C_3H_6 light-off temperature and the N_2
18 selectivity of the TPSR and the reverse TPSR decrease from 298 to 237°C (Table 3) and from
19 70 to 30%, respectively. On the other hand, the conversion of NO_x to N_2 remains almost
20 constant and close to 9% at maximum NO_x conversion.

21 Such phenomena were not observed for the CZ-based catalysts for which the C_3H_6 and NO_x
22 profiles of the TPSR and the reverse TPSR were comparable.

23 As in the case of the $C_3H_6-O_2$ reaction, Table 3 shows that the C_3H_6 light-off
24 temperature for the TPSR is lowest for $Pd(0.93)/SiO_2$ and highest for CZ. Pd also promotes
25 significantly C_3H_6 oxidation for the CZ-based catalysts.

1 3.1.11. Steady-state NO-C₃H₆-O₂ reaction

2 Prior to steady-state measurements, the catalysts were submitted to a TPSR under the
3 complete reacting mixture from RT to 500°C with a heating rate of 10°C min⁻¹.

4 Fig. 10 shows the performances of the catalysts for the reduction of NO_x under steady-
5 state conditions with stepwise increase of the temperature. The temperature of maximum of
6 N₂ formation, the corresponding NO_x and C₃H₆ conversions are listed in Table 4.

7 It is obvious that the introduction of Pd leads to a significant increase of NO_x
8 reduction to N₂ as well as a drastic decrease of the C₃H₆ light-off temperature. Table 3 lists
9 the temperature of light-off of C₃H₆ over various Pd-containing catalysts with respect to
10 reaction conditions. From this table it can also be concluded that the presence of NO does not
11 influence this light-off temperature, as was the case for CZ ([38] and first line of Table 3).

12 Conversion of NO_x to N₂ higher than 20% is obtained on the Pd/CZ catalysts. On the
13 other hand, Pd(0.93)/SiO₂ shows a rather low conversion of NO_x to N₂ close to that found for
14 CZ, despite the fact that the light-off temperature of propene is similar to that of the most
15 active CZ-based catalyst (Pd(0.89)/CZ). One also may note that propene oxidation is steeper
16 over Pd(0.93)/SiO₂ than over Pd/CZ catalysts. It is worthwhile noting that N₂ selectivity is
17 higher than 80% on CZ-based catalysts, whereas that of Pd(0.93)/SiO₂ is of 28% (Table 4).
18 Finally, Fig. 10e shows that NO oxidation to NO₂ is almost eliminated in the presence of
19 C₃H₆ before 400°C, the temperature of which corresponds to the almost complete conversion
20 of C₃H₆ (Fig. 10c).

21 To illustrate the high stability of the CZ-supported catalysts, Table 5 reports on the
22 influence of time on stream on the reduction of NO_x on Pd(0.89)/CZ. This catalyst exhibits
23 NO_x conversion to N₂ by about 30% and does not deactivate in the absence of water for 1 h.
24 After about 1 hour of run, 1.7% of water was introduced in the reaction mixture. This addition
25 decreases the conversion of NO_x by about 10%. More interesting is that the catalyst does not

1 deactivate over a period of 19 hours on stream in the presence of water. After 19 hours on
2 stream, the initial activity is restored when water is removed from the feed. This suggests that
3 H₂O competes with the active sites responsible for N₂ formation. C₃H₆ conversion remains
4 almost unaffected and close to 60%. Chemical analysis of this sample after reaction reveals a
5 carbon content of only 0.4 wt%.

6

7 *3.1.12. Steady-state NO-C₃H₆-O₂ reaction over mechanical mixtures*

8 The results obtained over two mechanical mixtures of Pd(0.89)/CZ + SiO₂ and
9 Pd(0.93)/ SiO₂ + CZ are shown in Fig. 11. It is obvious that the mechanical mixture of
10 Pd(0.89)/CZ + SiO₂ (Fig. 11a) is more active than its counterpart (Fig. 11b) over a wide range
11 of temperature. Table 6 compares the performances of the mechanical mixtures at about
12 250°C. Given that SiO₂ exhibits no deNO_x, the activity reported for the mechanical mixture of
13 Pd(0.89)/CZ and SiO₂ is only due to Pd(0.89)/CZ. It is quite unusual to note that the HSV
14 does not influence the performance of the Pd(0.89)/CZ catalyst as the experiments carried out
15 with 0.10 or 0.20 g of this sample give comparable deNO_x activities (Table 4 and Table 6,
16 Fig. 10d and Fig. 11a). This unexpected result suggests that the geometry of the reactor used
17 in this study was not the best to achieve optimised deNO_x conversions. The deNO_x activity
18 reported for the mechanical mixture made up of Pd(0.93)/SiO₂ and CZ roughly corresponds to
19 the sum of the activities of both catalytic systems. These conclusions are corroborated by the
20 selectivity to N₂ that is: (i) close to that reported for Pd(0.89)/CZ (Table 4) for the mechanical
21 mixture made up of Pd(0.89)/CZ and SiO₂ (Table 6), and (ii) intermediate to those of
22 Pd(0.93)/SiO₂ and CZ (Table 4) for the corresponding mechanical mixture (Table 6).

23

24

25

1 3.1.13. Steady-state NO-C₃H₆OH-O₂ reaction over Ce_{0.68}Zr_{0.32}O₂

2 Over CZ, C₃H₆ was substituted by 1-C₃H₇OH as reductant. The results of this steady-
3 state experiment are shown in Fig. 12. In contrast to the steady-state measurements with C₃H₆
4 as reductant (Fig. 10b), CZ exhibits a higher lean deNO_x activity in the presence of
5 1-C₃H₇OH over a broader range of temperatures than with C₃H₆. In comparison, the highest
6 activity, 19% NO_x to N₂ at 283°C when 1-C₃H₇OH is used as reductant, is more than twice
7 that listed at 361°C with C₃H₆ (Table 4). The selectivity to N₂ in the presence of C₃H₇OH
8 (76%) is comparable to that found in the presence of C₃H₆ (81%).

10 4. Discussion

12 4.1. State of Pd in the supported Pd catalysts

13 The XRD pattern of the calcined Pd(0.93)/SiO₂ sample (Fig. 2) indicates, as expected,
14 the presence of PdO. The corresponding reduced sample exhibits propene hydrogenation
15 activity (Table 1).

16 As mentioned in the results (part 3.1.3.), due to the overlapping of the diffraction
17 peaks of PdO with those of CZ, XRD characterisation could not be successfully used to
18 investigate the nature of the Pd species of the Pd/CZ catalysts. XANES measurements of
19 oxidised and reduced Pd(0.54)/CZ samples show that they closely resemble those of PdO and
20 the Pd foil, respectively (Fig. 3). As in the case of Pd/SiO₂, these XANES measurements
21 suggest that Pd is present as PdO for the calcined sample (Fig. 3a). Pd/CZ catalysts also
22 catalyse propene hydrogenation (Table 1), which agrees fairly well with the XANES
23 measurements of the reduced Pd(0.54)/CZ sample (Fig. 3), indicating the presence of reduced
24 Pd clusters. Holles and Davis have reported, however, that Pd(4.0)/CeO_x/Al₂O₃ could not be
25 fully reduced even after exposure to CO at 400°C [68]. Comparable conclusions were also

1 drawn by Matsumara and coworkers for Pd(3.0)/CeO₂ and Pd(2.0)/ZrO₂ samples reduced
2 under H₂ at 300 and 400°C [69,70], respectively. As X-ray absorption spectroscopy is known
3 to provide an average picture of the targeted metal species [71], CO-FTIR measurements were
4 also performed on Pd(0.89)/CZ (Fig. 4b). In agreement with XANES measurements, CO-
5 FTIR spectra recorded after H₂ reduction at 500°C do not reveal the presence of Pd oxidised
6 species, as is the case with a CZ-supported Rh catalyst [58].

7 The characterisation of these catalysts after oxidising or reducing pretreatments were
8 motivated due to the initial calcination of the samples and the C₃H₆-NO-O₂ TPSR experiment
9 that was carried out before steady-state measurements, the TPSR experiment leading to the
10 exposure of the calcined sample to the C₃H₆ reductant. The characterisation of the Pd/CZ
11 catalysts indicates that Pd is present as PdO in the calcined samples. Nevertheless, one might
12 wonder about the nature of the Pd species in the course of the lean NO_x reaction. Fernàndez-
13 Garcia et al. have recently shown that even under a stoichiometric C₃H₆+CO+NO+O₂
14 mixture, Pd was not reduced to Pd⁰ for Pd(1.0)/Ce_{0.5}Zr_{0.5}O₂ up to reaction temperature as high
15 as 400°C, but remained in an oxidised state due to contact between PdO clusters and ceria-
16 zirconia [72]. It is, thus, very likely that the same conclusion also applies to the Pd/CZ
17 catalysts of the present work. This assumption is supported by: (i) the TPR traces revealing
18 greater interaction of the Pd species with CZ than with SiO₂ (Fig. 1), and (ii) the steady-state
19 catalytic results (Table 4 and Table 6) that show markedly different N₂ selectivity for Pd/CZ
20 and Pd/SiO₂ catalysts. The N₂ selectivity found over the Pd/CZ catalysts is, indeed, more than
21 twice that observed over Pd/SiO₂. The N₂ selectivity listed for Pd/SiO₂ agrees well with those
22 already reported over a comparable catalytic system [19], over Pd/Al₂O₃ [34] or over Pt⁰
23 clusters [19]. This means that PdO is reduced to Pd⁰ when being supported on SiO₂ even
24 under a lean atmosphere. Such a conclusion has also been reported by Fernàndez-Garcia et al.
25 for alumina-supported Pd catalysts [72]. As already mentioned above, however, these authors

1 have demonstrated that this was not the case for a Pd(1.0)/Ce_{0.5}Zr_{0.5}O₂ catalyst. The obvious
2 higher N₂ selectivity for the Pd/CZ catalysts might also suggest that the deNO_x mechanism
3 occurring over these materials is different from the dissociation mechanism reported over
4 zero-valent PGMs atoms [6,9] and, thus, that the nature of the Pd species of the Pd/CZ
5 catalysts is different from that of Pd⁰. These arguments are further supported by the
6 comparison of the light-off of C₃H₆ of the TPSR and reverse TPSR (see part 3.1.10.) that
7 decreases to a significant extent on Pd(0.93)/SiO₂, and it is hardly affected at all on Pd/CZ
8 catalysts. Under the experimental conditions of the present study, it is, therefore, very likely
9 that Pd is present as PdO_x species, with x close to unity [73], rather than Pd⁰.

10

11 *4.2. Lean deNO_x mechanism proposal over PdO_x/CZ catalysts*

12 The results of the present work show that the incorporation of Pd to CZ promotes
13 significantly lean deNO_x activity (Fig. 10). In addition, CZ-supported catalysts exhibit a much
14 higher N₂ selectivity compared with that of Pd⁰(0.93)/SiO₂ (Table 4). Centi et al. [31] and
15 Liotta et al. [32] have also recently reported elevated N₂ selectivities over Pt/Ce_{0.60}Zr_{0.40}O₂-
16 Al₂O₃ and Pt/Ce_{0.60}Zr_{0.40}O₂ catalysts. These authors, however, did not comment about this
17 peculiarity. As already mentioned in the preceding characterisation section, this obvious
18 difference in N₂ selectivity between Pd⁰/SiO₂ and PdO_x/CZ catalysts suggests that the lean
19 deNO_x mechanism occurring over PdO_x/CZ catalysts is different from that occurring over
20 Pd⁰/SiO₂. The fairly low N₂ selectivity found for Pd⁰/SiO₂ (Table 4) indicates that lean deNO_x
21 most likely proceeds through the NO dissociation mechanism [9] on zero-valent Pd clusters,
22 the oxygen left from NO dissociation on the reduced surface being "cleaned" by the C₃H₆
23 oxidation reaction.

24 In a recent article [38], we suggested that reaction intermediates such as NO₂, organic
25 nitrogen-containing compounds (RNO_x) and oxygenates (C_xH_yO_z) might be involved in the

1 lean deNO_x catalysis on CZ. In the proposed mechanism, the production of NO₂ and C_xH_yO_z,
2 the formation of the latter resulting from the decomposition of R-NO_x intermediates produced
3 by the reaction of NO₂ and C₃H₆, has been assumed to be critical for lean deNO_x activity, as
4 also reported by other authors [34]. The present study also shows that NO oxidation to NO₂ is
5 achieved on the bare support, as the introduction of Pd does not promote such a reaction (Fig.
6 5). This conclusion is consistent with the work of Krishna et al. in which the authors reported
7 that CeO₂ is a fairly efficient catalyst in the oxidation of NO [74].

8 The activation of C₃H₆ proceeds unambiguously on the PdO_x catalytic function, as
9 demonstrated by the C₃H₆ light-off temperature that decreases significantly over supported Pd
10 catalysts (Fig. 10 and Table 3). In addition, it is obvious that this low temperature activation
11 of C₃H₆ is responsible for the lean deNO_x activity of PdO_x/CZ catalysts, as both C₃H₆
12 activation and deNO_x occur concomitantly (Fig. 9 and Fig. 10c,d).

13 One might, however, wonder about the activation process of C₃H₆ in the course of the
14 deNO_x reaction. On that point, the TPD in C₃H₆-O₂ after adsorption of NO-O₂ is very
15 informative. Fig. 7b shows that C₃H₆ is activated through ad-NO₂ species, as already
16 proposed on CZ [38], the low temperature (130-180°C) consumption of C₃H₆ being different
17 from the C₃H₆ profiles observed in the C₃H₆-O₂ reaction on Pd(0.89)/CZ (Fig. 8) and in the
18 TPD in C₃H₆-O₂ after adsorption of NO-O₂ on CZ (Fig. 7a). In this temperature range, it is
19 worthwhile noting that the NO₂ concentration of the TPD in N₂ after adsorption of NO-O₂ on
20 Pd(0.89)/CZ is greater than that of CZ (Fig. 6c, 130-180°C region). These observations
21 strongly suggest that NO₂ species adsorbed on the PdO_x catalytic function account for the
22 activation of C₃H₆. Such a conclusion is also supported by the fact that NO is mainly
23 desorbed in the TPD in C₃H₆-O₂ after adsorption of NO-O₂ (Table 2), whereas NO₂ would
24 have been expected to be the most abundant desorbed compound from the TPD in N₂ (Table 2
25 and Fig. 6b). As discussed previously [38], the activation of C₃H₆ by ad-NO₂ and the

1 concomitant release of NO might be attributed to the intermediate formation of R-NO_x
2 compounds, the decomposition of which produces NO and C_xH_yO_z.

3 One might wonder whether lean deNO_x also occurs on the PdO_x catalytic function.
4 Given that lean deNO_x occurs to a significant extent on CZ when C₃H₆ is substituted by 1-
5 C₃H₇OH (Fig. 12), it seems more likely that NO reduction takes place via a lacunar
6 mechanism on reduced CZ sites, as proposed by several groups [75-78]. These authors,
7 indeed, provided evidence for the decomposition of NO to N₂ on prerduced CeO₂ surfaces. It
8 is worth reporting that this decomposition pathway has also been considered in Three-Way
9 Catalysis in which CO is used as reductant [15]. In the course of the lean deNO_x reaction, the
10 creation of the sites responsible for the decomposition of NO would, thus, be achieved by
11 reduction of CZ by the oxygenates (C_xH_yO_z) produced by the decomposition of R-NO_x
12 formed on the PdO_x catalytic function.

13 The corresponding detailed mechanism of the C₃H₆-assisted decomposition of NO on
14 PdO_x/CZ catalysts is described in Fig. 13. This mechanism stresses the key role of NO₂, R-
15 NO_x and C_xH_yO_z as intermediates of the Selective Catalytic Reduction (SCR) of NO_x by
16 hydrocarbons, as also suggested in many studies [34,38 and references therein]. The proposed
17 mechanism is consistent with previous studies of Djega-Mariadassou [16,79] who reported
18 that three catalytic functions were required for the occurrence of the SCR of NO_x by
19 hydrocarbons. In this model, CZ achieves both NO oxidation to NO₂ (cycle 1) and NO
20 decomposition to N₂ (cycle 3), whereas PdO_x activates C₃H₆ via ad-NO₂ species (cycle 2)
21 intermediately producing R-NO_x compounds that further decompose to NO and C_xH_yO_z. The
22 role of the latter oxygenates is to reduce CZ to provide the catalytic sites responsible for NO
23 decomposition (catalytic cycle 3). In the proposed mechanism, the reaction of NO₂ with C₃H₆
24 to give NO back and the competition between the NO oxidation and decomposition reactions
25 on the CZ catalytic sites also account for the limited formation of NO₂ in the course of the

1 lean deNO_x process (Fig. 7b, Fig. 9 and Fig. 10e). At elevated temperatures, complete
2 oxidation of C₃H₆ by molecular O₂ becomes predominant [80] on PdO_x, and the deNO_x
3 process cannot proceed further.

4

5 **5. Conclusion**

6 This study shows that the incorporation of Pd to CZ greatly promotes the reduction of
7 NO in the presence of C₃H₆. These catalysts display very stable deNO_x activity even in the
8 presence of 1.7% water, the addition of which induces a reversible deactivation of about 10%.

9 Ex situ characterisation of the catalysts through propene hydrogenation reaction, XRD,
10 XANES, CO absorption followed by FTIR along with the catalytic results indicate that PdO is
11 reduced to Pd⁰ clusters on Pd/SiO₂, this catalyst having been studied as a reference catalyst.
12 This complete reduction process, however, does not occur for PdO_x/CZ catalysts under our
13 experimental conditions.

14 The PdO_x/CZ catalysts also exhibit much higher selectivity to N₂ than that of
15 Pd⁰/SiO₂, the selectivity of which is consistent with those already reported in literature data
16 over supported zero-valent noble metal catalysts. The much higher N₂ selectivity obtained on
17 PdO_x/CZ suggests that the lean deNO_x mechanism occurring on these catalysts is different
18 from that occurring on Pd⁰/SiO₂ which consists of the dissociation of NO on reduced
19 palladium sites, followed by the regeneration of the active Pd⁰ sites by C₃H₆. The results of
20 the catalytic experiments led us to propose a detailed mechanism (Fig. 13) for which CZ
21 achieves both NO oxidation to NO₂ and NO decomposition to N₂, whereas PdO_x activates
22 C₃H₆ via ad-NO₂ species, intermediately producing R-NO_x compounds that further
23 decompose to NO and C_xH_yO_z. The role of the latter oxygenates is to reduce CZ to provide
24 the catalytic sites responsible for NO decomposition. Finally, the proposed C₃H₆-assisted NO

1 decomposition mechanism stresses the key role of NO₂, R-NO_x and C_xH_yO_z as intermediates
2 of the Selective Catalytic Reduction (SCR) of NO_x by hydrocarbons.

3

4 **Acknowledgments**

5 Rhodia contributed to part of the financial support for this work; the Ministère de
6 l'Enseignement Supérieur et de la Recherche organization supported the work of Dr. Gorce
7 (Grant 98-4-10713) and Ms Fontaine (Grant 8449-2003). We also thank G. Blanchard for his
8 interest in this work and P. Lavaud for his invaluable help in technical support.

9

10 **References**

11

- [1] K.C. Taylor, in *Catalysis Science and Technology*, J.R. Anderson, M. Boudart, Automobile Catalytic Converters, Springer-Verlag, Berlin, 1982, p. 119.
- [2] M. Shelef, G.W. Graham, *Catal. Rev. Sci. Eng.* 36 (1994) 431.
- [3] M.D. Amiridis, T. Zhang, R.J. Farrauto, *App. Catal. B: Env.* 10 (1996) 203.
- [4] V.I. Pârvulescu, P. Grange, B. Delmon, *Catal. Today* 46 (1998) 233.
- [5] R.J. Farrauto, R.M. Heck, *Catal. Today* 51 (1999) 351.
- [6] R. Burch, J.P. Breen, F.C. Meunier, *Appl. Catal. B: Env.* 39 (2002) 283.
- [7] F. Fajardie, J.-F. Tempère, J.-M. Manoli, O. Touret, G. Blanchard, G. Djéga-Mariadassou, *J. Catal.* 179 (1998) 469.
- [8] T.W. Root, L.D. Schmidt, G.B. Fischer, *Surf. Sci.* 134 (1983) 30.
- [9] R. Burch, P.J. Millington, A.P. Walker, *Appl. Catal. B: Env.* 4 (1994) 65.
- [10] R. Burch, P.K. Loader, N.A. Cruise, *Appl. Catal. A: Gen.* 147 (1996) 375.
- [11] N. Miyoshi, S. Matsumoto, K. Katoh, T. Tanaka, J. Harada, N. Takahashi, K. Yokota, M. Sugiura, K. Kasahara, SAE 950809, 1995.

- [12] M. Iwamoto, H. Furukawa, Y. Mina, F. Uemura, S. Mikuriya, S. Kagawa, *J. Chem. Soc. Chem. Com.* (1986) 1275.
- [13] M. Iwamoto, K. Maruyama, N. Yamazoe, T. Seiyama, *J. Chem. Soc. Chem. Com.* (1966) 615.
- [14] Y. Lee, J.N. Armor, *App. Catal.* 76 (1995) L1.
- [15] G. Djéga-Mariadassou, F. Fajardie, J.-F. Tempère, J.-M. Manoli, O. Touret, G. Blanchard, *J. Mol. Catal. A: Chem.* 161 (2000) 179.
- [16] G. Djéga-Mariadassou, *Catal. Today* 90 (2004) 27.
- [17] S. Matsumoto, K. Yokota, H. Doi, M. Kimura, S. Kasahura, *Catal. Today* 22 (1994) 127.
- [18] K. Yogo, M. Umeno, H. Watanabe, E. Kikuchi, *Catal. Lett.* 19 (1993) 131.
- [19] R. Burch, P.J. Millington, *Catal. Today* 29 (1996) 37.
- [20] G.R. Bamwenda, A. Ogata, A. Obuchi, J. Oi, K. Mizuno, J. Skrzypek, *Appl. Catal. B: Env.* 6 (1995) 311.
- [21] J. Li, J. Hao, L. Fu, T. Zhu, *Topics Catal.* 30/31 (2004) 81.
- [22] T. Tanaka, T. Okuhara, M. Misono, *Appl. Catal. B: Env.* 4 (1994) L1.
- [23] R. Burch, T.C. Watling, *Catal Lett.* 37 (1996) 51.
- [24] R. Burch, T.C. Watling, *Catal Lett.* 43 (1997) 19.
- [25] T. Okuhara, Y. Hasada, M. Misono, *Catal. Today* 35 (1997) 83.
- [26] R. Burch, T.C. Watling, *Appl. Catal. B: Env.* 11 (1997) 207.
- [27] R. Burch, J.A. Sullivan, T.C. Watling, *Catal. Today* 42 (1998) 13.
- [28] E. Joubert, T. Bertin, J.C. Ménézo, J. Barbier, *Appl. Catal. B: Env.* 23 (1999) L83.
- [29] D.K. Captain, K.L. Roberts, M.D. Amiridis, *Catal. Today* 42 (1998) 93.
- [30] P. Denton, A. Giroir-Fendler, H. Praliaud, M. Primet, *J. Catal.* 189 (2000) 410.

- [31] G. Centi, P. Fornasiero, M. Graziani, J. Kašpar, F. Vazzana, *Topics Catal.* 16/17 (2001) 157.
- [32] L.F. Liotta, A. Longo, A. Macaluso, A. Martorana, G. Pantaleo, A.M. Venezia, G. Deganello, *Appl. Catal. B: Env.* 48 (2004) 133.
- [33] A. Obuchi, A. Ogata, H. Takahashi, J. Oi, G.R. Bamwenda, K. Mizuno, *Catal. Today* 29 (1996) 103.
- [34] K.O. Haj, S. Ziyade, M. Ziyad, F. Garin, *Appl. Catal. B: Env.* 37 (2002) 49.
- [35] Y. Traa, B. Burger, J. Weitkamp, *J. Chem. Soc. Chem. Comm.* 21 (1999) 2187.
- [36] P. Degobert, *Automobiles and Pollution* (Institut Français du Pétrole Publications, Editions Technip, Paris 1995)
- [37] S.N. Orlik, V.L. Struzhko, T.V. Mironyuk, G.M. Tel'biz, *Theor. Exp. Chem.* 37 (2001) 311.
- [38] O. Gorce, F. Baudin, C. Thomas, P. Da Costa, G. Djéga-Mariadassou, *Appl. Catal. B: Env.* 54 (2004) 69.
- [39] R. Rajasree, J.H.B.J. Hoebink, J.C. Shouten, *J. Catal.* 223 (2004) 36.
- [40] N. Hickey, P. Fornasiero, R. Di Monte, J. Kašpar, J.R. González-Velasco, M.A. Gutiérrez-Ortiz, M.P. González-Marcos, J.M. Gatica, S. Bernal, *J. Chem. Soc., Chem. Commun.* (2004) 196.
- [41] S. Bedrane, C. Descorme, D. Duprez, *Catal. Today* 75 (2002) 41.
- [42] S. Salasc, V. Perrichon, M. Primet, N. Mouaddib-Moral, *J. Catal.* 206 (2002) 82.
- [43] A. Iglesia-Juez, A. Martínez-Arias, M. Fernández-García, *J. Catal.* 221 (2004) 148.
- [44] C. Bozo, N. Guilhaume, J.-M. Herrmann, *J. Catal.* 203 (2001) 393.
- [45] G. Pecchi, P. Reyes, R. Zamora, T. Lopez, R. Gomez, *J. Chem. Tech. Biotech.* 80 (2005) 268.

- [46] J. Breen, R. Burch, H.M. Coleman, *Appl. Catal. B: Env.* 39 (2002) 65.
- [47] S.H. Overbury, D.R. Mullins, in *Catalysis by Ceria and Related Materials*, A. Trovarelli (Ed.), *Ceria Surfaces and Films for Model Catalytic Studies Using Surface Analysis Techniques*, Imperial College Press, London, 2002, p.328.
- [48] L. Salin, C. Potvin, J.-F. Tempère, M. Boudart, G. Djéga-Mariadassou and J.-M. Bart, *Ind. Eng. Chem. Res.* 37 (1998) 4531.
- [49] A. Michalowicz, *Logiciels pour la chimie; Société Française de Chimie*, Paris (1991) 102.
- [50] A. Michalowicz, *J. Phys. IV France* 7 (1997) 235.
- [51] C. de Leitenburg, A. Trovarelli, J. Kašpar, *J. Catal.* 166 (1997) 98.
- [52] H.-W. Jen, G.W. Graham, W. Chun, R.W. McCabe, J.-P. Cuif, S.E. Deutsch, O. Touret, *Catal. Today* 50 (1999) 309.
- [53] R. Di Monte, P. Fornasiero, M. Graziani, J. Kašpar, *J. Alloys Comp.* 275-277 (1998) 877.
- [54] P. Fornasiero, N. Hickey, J. Kašpar, T. Montini, M. Graziani, *J. Catal.* 189 (2000) 339.
- [55] P. Fornasiero, J. Kašpar, M. Graziani, *J. Catal.* 167 (1997) 576.
- [56] M.-F. Luo, X.-M. Zheng, *Appl. Catal. A: General* 189 (1999) 15.
- [57] P. Fornasiero, R. Di Monte, G. Ranga Rao, J. Kašpar, S. Meriani, A. Trovarelli, M. Graziani, *J. Catal.* 151 (1995) 168.
- [58] C. Fontaine, C. Thomas, J.-M. Krafft, O. Gorce, F. Villain, G. Djéga-Mariadassou, *in preparation*.
- [59] K. Hadjiivanov, G.N. Vayssilov, *Adv. Catal.* 47 (2002) 307.
- [60] J.-C. Lavalley, J. Saussey, J. Lamotte, R. Breault, J. P. Hindermann, A. Kiennemann, *J. Phys. Chem.* 94 (1990) 5941.

- [61] A. Badri, C. Binet, J.-C. Lavalley, *J. Phys. Chem.* 100 (1996) 8363.
- [62] A. Badri, C. Binet, J.-C. Lavalley, *J. Chem. Soc., Farad. Trans.* 92 (1996) 1603.
- [63] A. Bensalem, J.-C. Muller, D. Tessier, F. Bozon-Verduraz, *J. Chem. Soc., Farad. Trans.* 92 (1996) 3233.
- [64] C. Force, J. P. Belzunegui, J. Sanz, A. Martínez-Arias, J. Soria, *J. Catal.* 197 (2001) 192.
- [65] K.I. Choi, M.A. Vannice, *J. Catal.* 127 (1991) 465.
- [66] L. Sordelli, G. Matra, R. Psaro, S. Coluccia, *J. Chem. Soc., Dalton Trans.* 5 (1996) 765.
- [67] M. Ogura, M. Hayashi, S. Kage, M. Matsukata, E. Kikuchi, *Appl. Catal. B: Env.* 23 (1999) 247.
- [68] J.H. Holles, R.J. Davis, *J. Phys. Chem. B* 104 (2000) 9653.
- [69] W.-J. Shen, Y. Ichihashi, M. Okumara, Y. Matsumara, *Catal. Lett.* 64 (2000) 23.
- [70] Y. Matsumara, M. Okumara, Y. Usami, K. Kagawa, H. Yamashita, M. Anpo, M. Haruta, *Catal. Lett.* 44 (1997) 189.
- [71] M. Vaarkamp, D.C. Koningsberger, in G. Ertl, H. Knözinger, J. Weitkamp (Ed.), *Handbook of Heterogeneous Catalysis*, Wiley-VCH, Weinheim, 1997, Vol. 2, p. 475.
- [72] M. Fernández-García, A. Iglesia-Juez, A. Martínez-Arias, A.B. Hungría, J.A. Anderson, J.C. Conesa, J. Soria, *J. Catal.* 221 (2004) 594.
- [73] T. Maillet, C. Solleau, J. Barbier Jr., D. Duprez, *Appl. Catal. B: Env.* 14 (1997) 85.
- [74] K. Krishna, M. Makkee, *Appl. Catal. B: Env.* 59 (2005) 35.
- [75] M. Niwa, Y. Furukawa, Y. Murakami, *J. Coll. Int. Sci.* 86 (1982) 260.
- [76] A. Martinez-Arias, J. Soria, J.C. Conesa, X.L. Soane, A. Arcoya, R. Cataluna, *J. Chem. Soc. Faraday. Trans.* 91 (1995) 1679.

- [77] S.H. Overbury, D.R. Mullins, D.R. Huntley, Lj. Kundakovic, *J. Catal.* 186 (1999) 296.
- [78] M. Daturi, N. Bion, J. Saussey, J.-C. Lavalley, C. Hedouin, T. Seguelon, G. Blanchard, *Phys. Chem. Chem. Phys.* 3 (2001) 252.
- [79] G. Djéga-Mariadassou, M. Boudart, *J. Catal.* 216 (2003) 89.
- [80] J. Haber, W. Turek, *J. Catal.* 190 (2000) 320.

Table 1: Determination of the percentage of exposed zero-valent Pd atoms (Pd^0) over $\text{Ce}_{0.68}\text{Zr}_{0.32}\text{O}_2$ (CZ)- and silica-supported catalysts by means of propene hydrogenation reactions [48].

Catalysts	Pd(0.54)/CZ	Pd(0.89)/CZ	Pd(0.93)/SiO ₂
Pd^0 (%)	17	16	22

Table 2: Amounts of adsorbed or desorbed NO_x (NO+ NO₂) and desorbed N₂O in the course of the TPD experiments after exposure of the catalysts to NO-O₂ (340 ppm – 8%) in N₂

Catalysts	experiment	Amounts of adsorbed (ads.) or desorbed (des.) species (10 ⁻⁵ mol g ⁻¹)					
		NO _{x ads.}	NO _{des.}	NO _{2 des.}	NO _{x des.}	N ₂ O _{des.}	N balance*
Ce _{0.68} Zr _{0.32} O ₂ (CZ)	TPD in N ₂	54.8	8.1	46.5	54.6	0.0	0.1
	TPD in C ₃ H ₆ -O ₂	48.2	19.0	7.8	26.8	5.8	4.9
Pd(0.89)/CZ	TPD in N ₂	47.6	6.2	36.4	42.7	0.0	2.5
	TPD in C ₃ H ₆ -O ₂	51.8	20.3	5.1	25.4	5.4	7.8

* N balance calculated with respect to N₂ equivalent

Table 3: C₃H₆ light-off temperatures (°C) of Ce_{0.68}Zr_{0.32}O₂ (CZ)- and silica-supported catalysts; 340ppm NO, 8% O₂, 1900 ppm C₃H₆ and N₂ balance

	Ads NO-O ₂	Transient	Transient	Steady-state
	TPD in O ₂ -C ₃ H ₆	O ₂ -C ₃ H ₆	NO-O ₂ -C ₃ H ₆	NO-O ₂ -C ₃ H ₆
CZ	450	473	387	380
Pd(0.54)/CZ	-	277	276	303
Pd(0.89)/CZ	276	251	252	243
Pd(0.93)/SiO ₂	-	-	298*	-
		236	237	237

* Light-off temperature measured in the course of the first NO-O₂-C₃H₆ TPSR

Table 4: Temperature of maximum of N₂ formation and percentage of NO_x converted to N₂ at this temperature over Ce_{0.68}Zr_{0.32}O₂ (CZ)-and silica-supported catalysts for the steady-state NO-O₂-C₃H₆ reaction (340 ppm - 8 % -1900 ppm, N₂ balance)

Catalysts	CZ	Pd(0.54)/CZ	Pd(0.89)/CZ	Pd(0.93)/SiO ₂
Sample Weight (g)	0.20	0.20	0.20	0.07
T max N ₂ (°C)	361	263	243	243
Conversion of NO _x to N ₂ (%)	8	21	29	7
Selectivity to N ₂ (%)*	81	83	87	28
C ₃ H ₆ conversion (%)	34	38	50	58

* Selectivity to N₂ referred to as $(N_2/(N_2 + N_2O) \times 100)$

Table 5: Influence of the addition of 1.7% water on the conversions of C₃H₆ and NO_x to N₂ at 278°C in the course of the C₃H₆-NO-O₂ reaction (1900 ppm- 340 ppm – 8 %, balance N₂) versus time on stream on Pd(0.89)/Ce_{0.68}Zr_{0.32}O₂.

	Time on stream (h)			
	0	1	20	20.5
H ₂ O (%)	0	1.7	1.7	0
Conversion of NO _x to N ₂ (%)	27	24	25	29
Selectivity to N ₂ (%)*	75	76	76	77
C ₃ H ₆ conversion (%)	65	62	62	60

* Selectivity to N₂ referred to as (N₂/(N₂ + N₂O) x 100)

Table 6: Percentage of NO_x converted to N₂ over Ce_{0.68}Zr_{0.32}O₂ (CZ)-and silica-supported catalysts for the steady-state NO-O₂-C₃H₆ reaction (340 ppm- 8 % -1900 ppm, N₂ balance)

Catalysts	Pd(0.89)/CZ + SiO ₂	Pd(0.93)/SiO ₂ + CZ
Sample Weight (g)	0.10 + 0.10	0.10 + 0.10
T (°C)	250	255
Conversion of NO _x to N ₂ (%)	29	12
Selectivity to N ₂ (%)*	86	51
C ₃ H ₆ conversion (%)	47	50

* Selectivity to N₂ referred to as $(N_2/(N_2 + N_2O) \times 100)$

Figure captions

Fig. 1: Temperature-Programmed Reduction profiles of the calcined (air 500°C, 2h) catalysts.

Fig. 2: XRD patterns of SiO₂, Pd(0.93)/SiO₂ and Ce_{0.68}Zr_{0.32}O₂.

Fig. 3: XANES spectra at the Pd K edge for PdO (▲), the Pd foil (Δ) and Pd(0.54)/CZ (oxidized in air at 500°C: ---- or reduced in H₂ at 500°C: —).

Fig. 4: FT infrared spectra of (a) Ce_{0.68}Zr_{0.32}O₂ (CZ) and (b) Pd(0.89)/CZ, reduced under flowing H₂ at 500°C for 2h and evacuation at 500°C for 1h, after introduction of equilibrated pressures of 0.9 (---) and 18 (—) torr of CO.

Fig. 5: Steady-state catalytic conversion of NO oxidation to NO₂ in the course of the NO-O₂ reaction (340 ppm - 8%, balance N₂): (◆) Ce_{0.68}Zr_{0.32}O₂ (CZ), (●) Pd(0.54)/CZ.

Fig. 6: NO_x Temperature-Programmed Desorption profiles in N₂ after exposure of the catalysts to NO-O₂ (340 ppm - 8%, balance N₂) at RT: (a) Ce_{0.68}Zr_{0.32}O₂ (CZ), (b) Pd(0.89)/CZ and (c) their comparison, the NO_x TPD of Pd(0.89)/CZ having been normalised with respect to the amount of NO_x adsorbed on CZ (Table 2).

Fig. 7: Temperature-Programmed Desorption profiles in $C_3H_6-O_2$ (1900 ppm – 8% O_2 , balance N_2) after exposure of the catalysts to $NO-O_2$ (340 ppm - 8%, balance N_2), at RT: (a) $Ce_{0.68}Zr_{0.32}O_2$ (CZ), (b) $Pd(0.89)/CZ$.

Fig. 8: Transient $C_3H_6-O_2$ (1900 ppm - 8% O_2 , balance N_2) reaction over $Pd(0.93)/SiO_2$ and $Pd(0.89)/Ce_{0.68}Zr_{0.32}O_2$.

Fig. 9: Temperature-Programmed Surface Reaction profiles of $C_3H_6-NO-O_2$ (1900 ppm - 340 ppm-8%) after exposure of $Pd(0.89)/Ce_{0.68}Zr_{0.32}O_2$ to $C_3H_6-NO-O_2$ (1900 ppm - 340 ppm - 8%, balance N_2) at RT.

Fig. 10: Steady-state catalytic conversions of C_3H_6 and NO_x to N_2 in the course of the $C_3H_6-NO-O_2$ reaction (1900 ppm- 340 ppm - 8%, balance N_2): (a) $Pd(0.93)/SiO_2$ (0.07g), (b) $Ce_{0.68}Zr_{0.32}O_2$ (CZ, 0.20g), (c) $Pd(0.54)/CZ$ (0.20g), (d) $Pd(0.89)/CZ$ (0.20g), and of NO to NO_2 over $Pd(0.54)/CZ$ (0.20g) (e): (●) $NO-O_2$ reaction (340 ppm - 8%, balance N_2), (○) $C_3H_6-NO-O_2$ reaction (1900 ppm- 340 ppm - 8%, balance N_2).

Fig. 11: Steady-state catalytic conversions of C_3H_6 and NO_x to N_2 in the course of the $C_3H_6-NO-O_2$ reaction (1900 ppm- 340 ppm - 8%, balance N_2) of mechanical mixtures: (a) $Pd(0.89)/Ce_{0.68}Zr_{0.32}O_2 + SiO_2$ (0.10g + 0.10g), (b) $Pd(0.93)/ SiO_2 + Ce_{0.68}Zr_{0.32}O_2$ (0.10g + 0.10g)

Fig. 12: Steady-state catalytic conversions of C_3H_7OH and NO_x to N_2 in the course of the $C_3H_7OH-NO-O_2$ reaction (2200 ppm- 340 ppm - 8%, balance N_2) over $Ce_{0.68}Zr_{0.32}O_2$ (CZ).

Fig. 13: (a) Schematic representation of the catalytic functions, (b) Mechanism of the lean C_3H_6 -assisted decomposition of NO over $Pd/Ce_{0.68}Zr_{0.32}O_2$ (CZ) catalysts, \boxed{O} , $R-NO_x$, $C_xH_yO_z$ representing an oxygen from the surface of the CZ support, organic nitrogen-containing and oxygenates compounds of undefined composition, respectively.

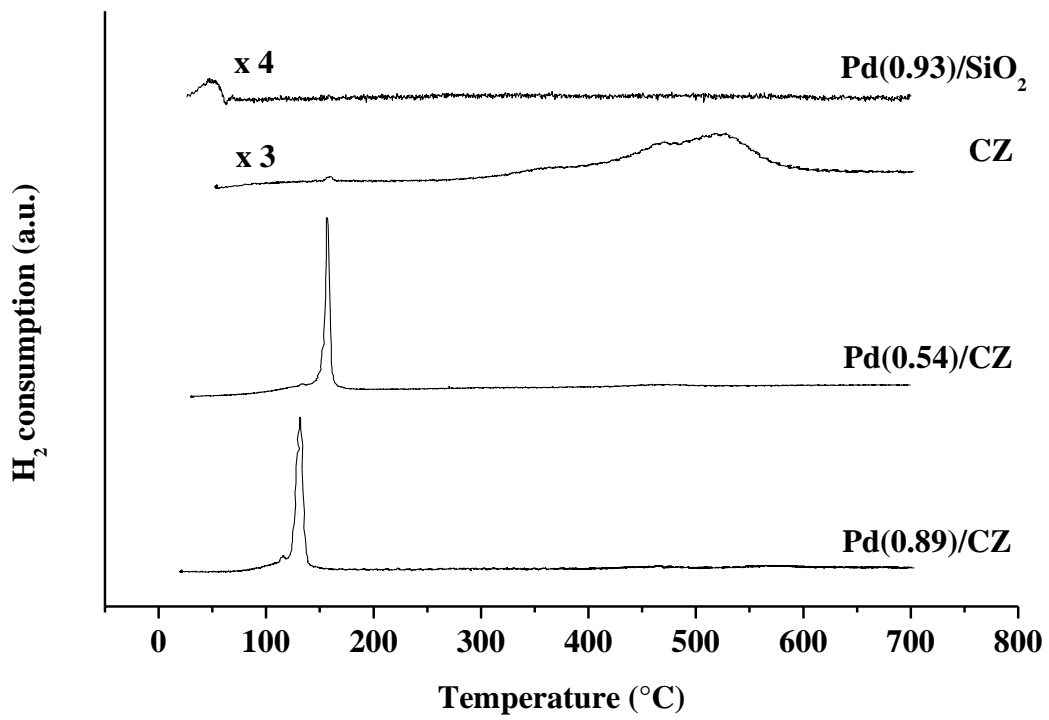


Fig. 1

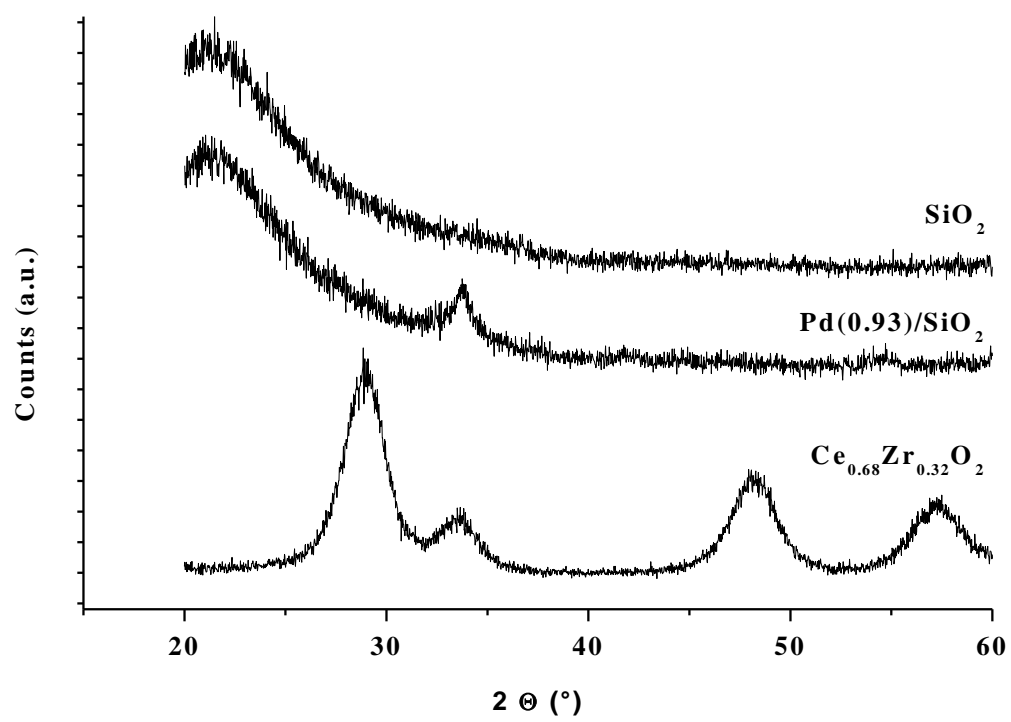


Fig. 2

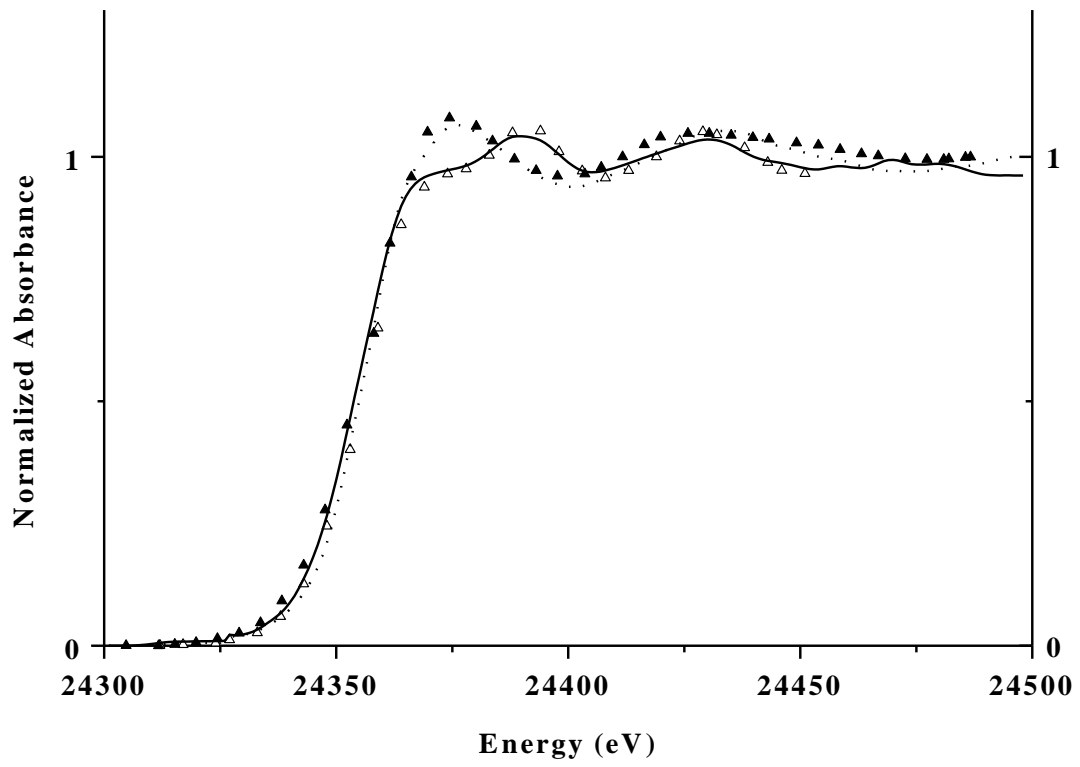


Fig. 3

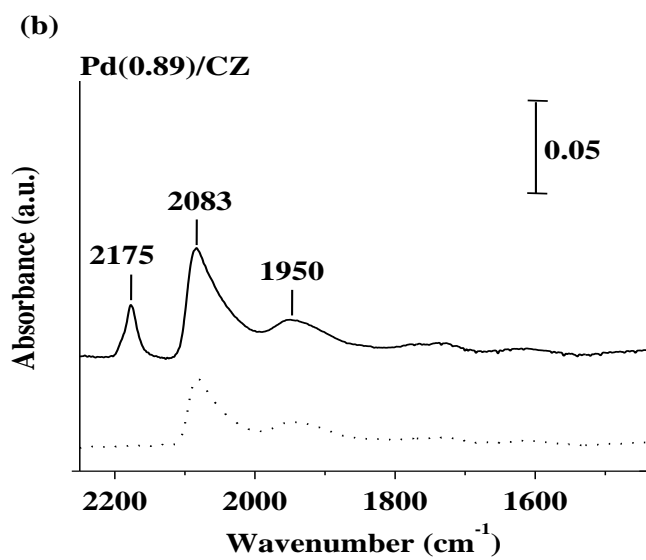
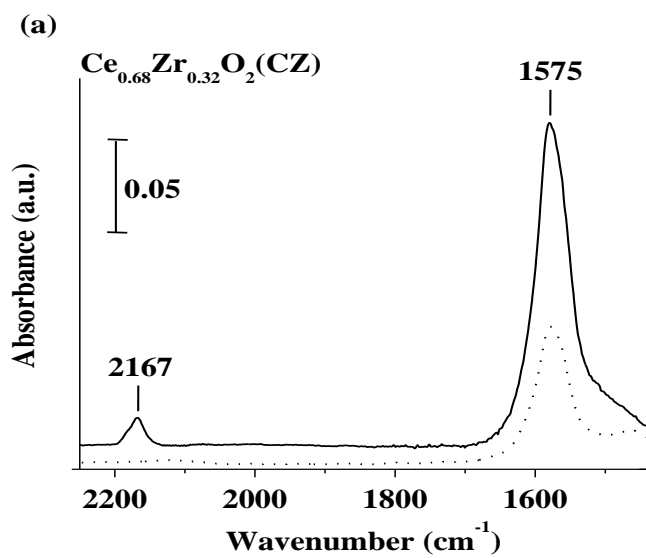


Fig. 4

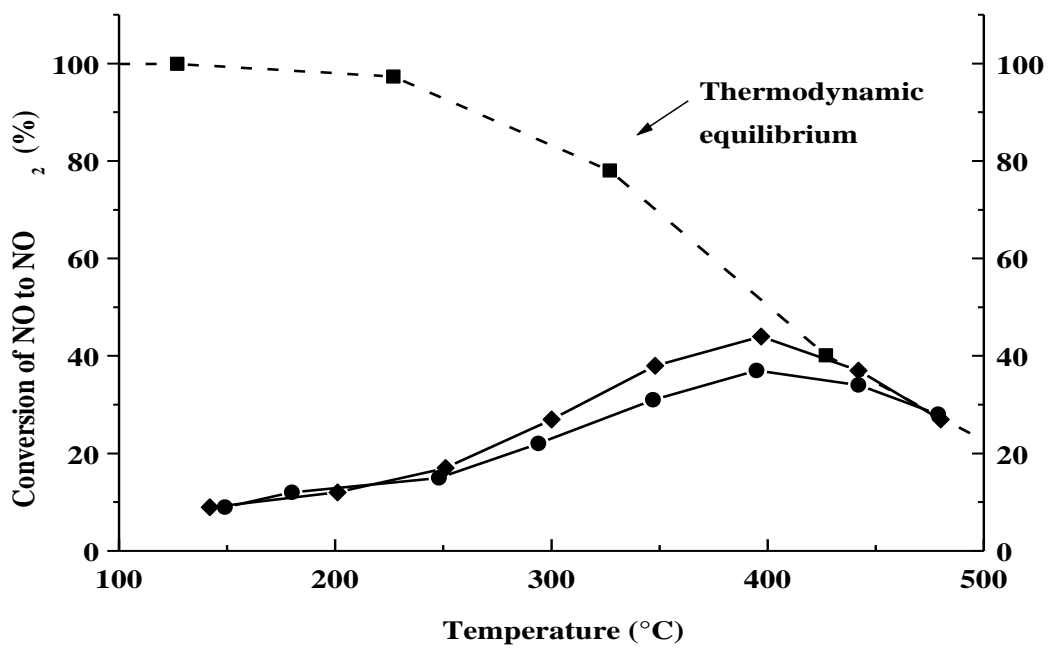


Fig. 5

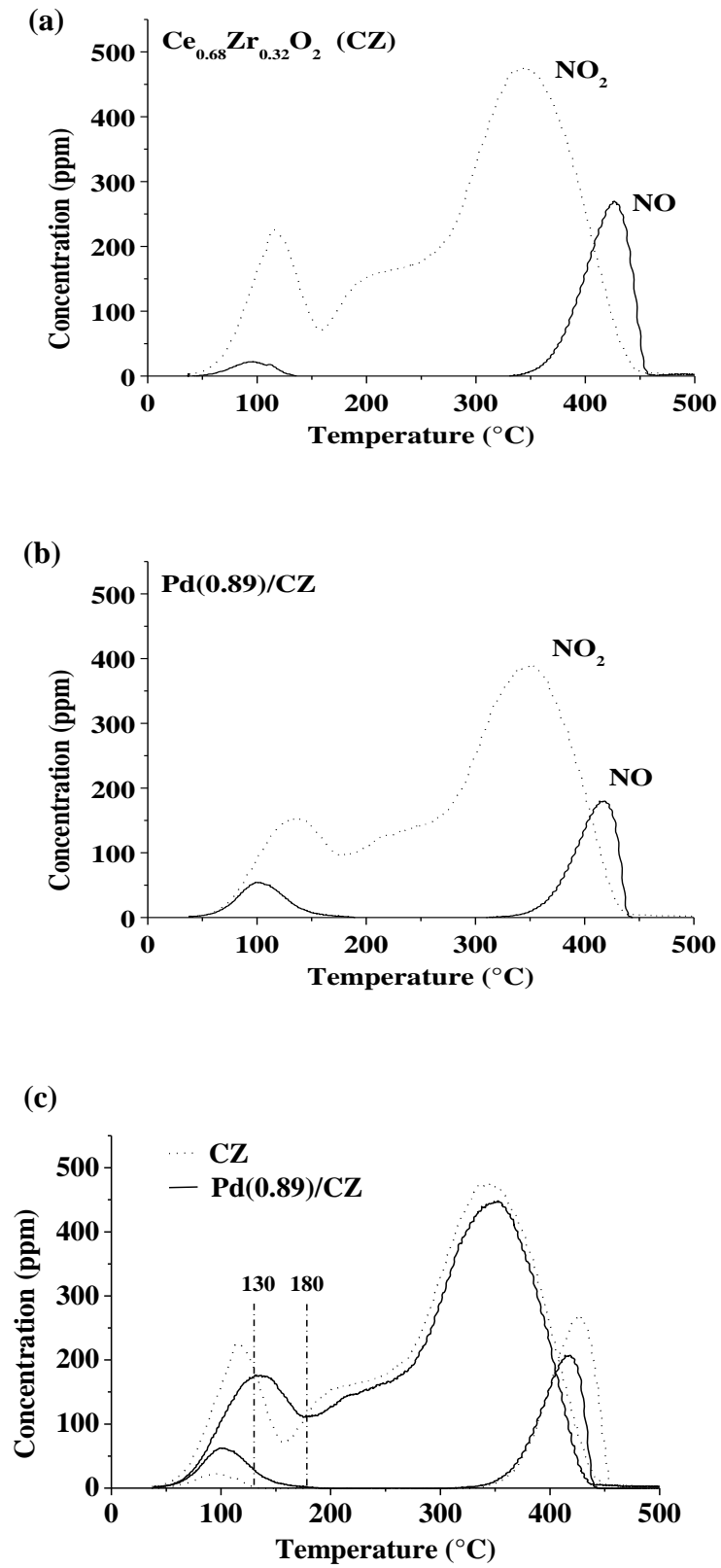


Fig. 6

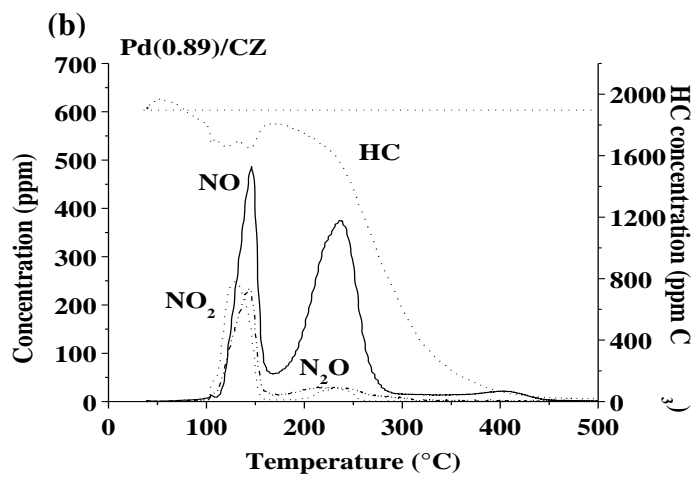
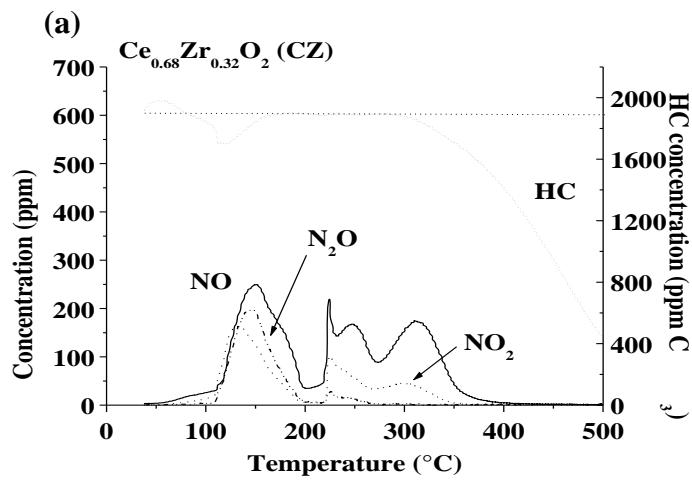


Fig. 7

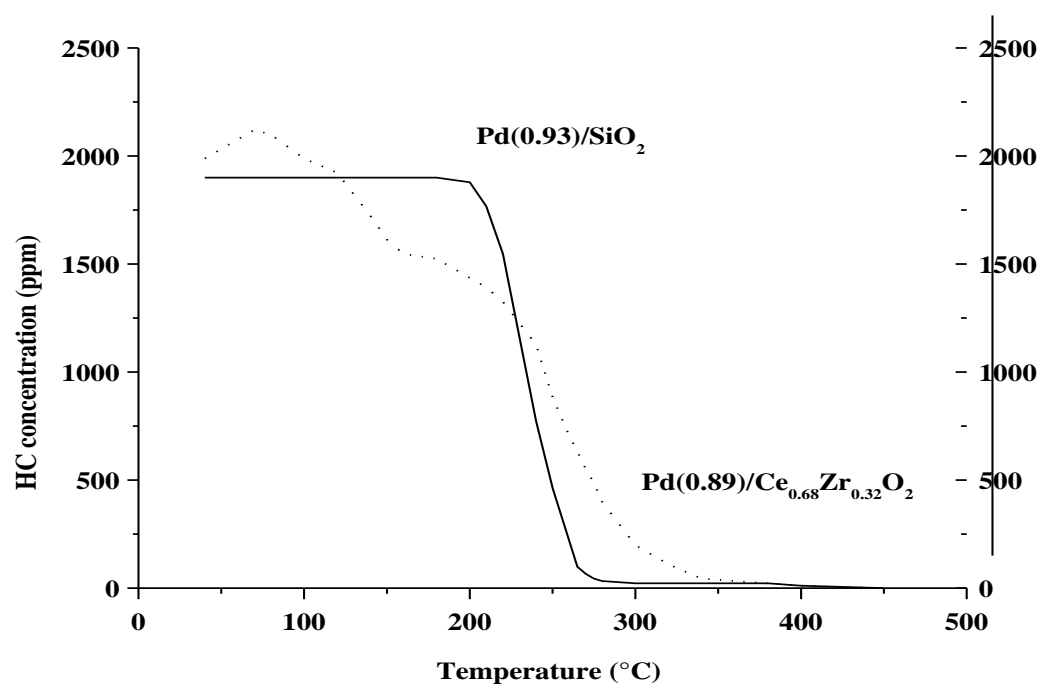


Fig. 8

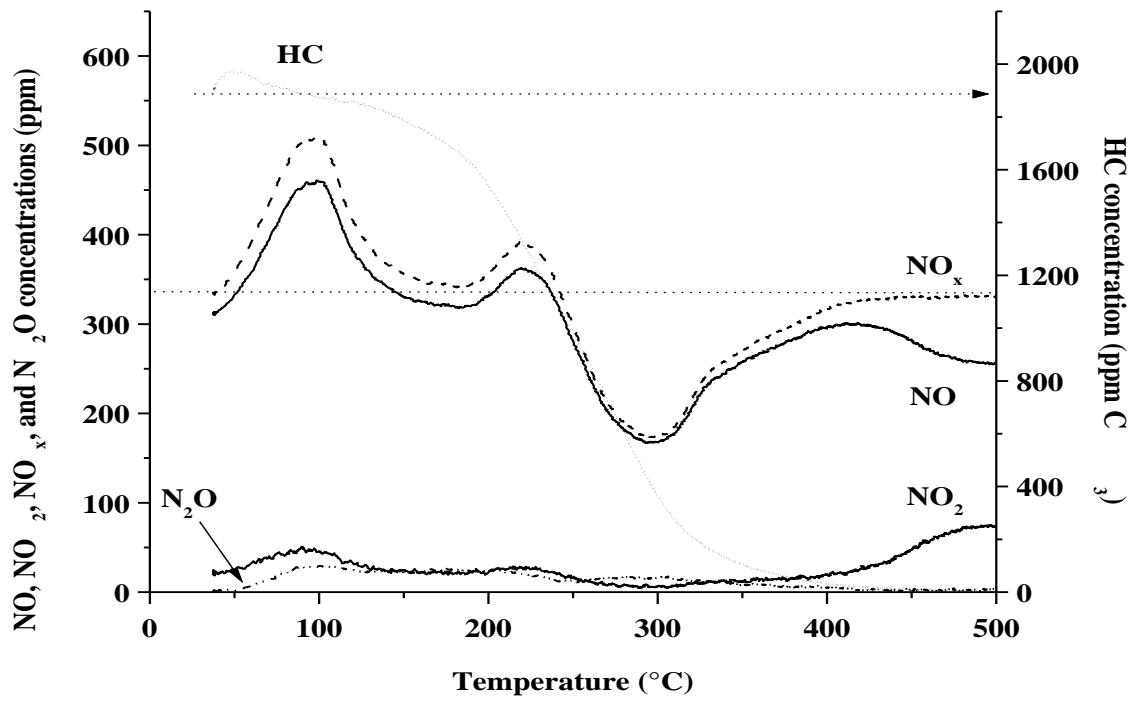


Fig. 9

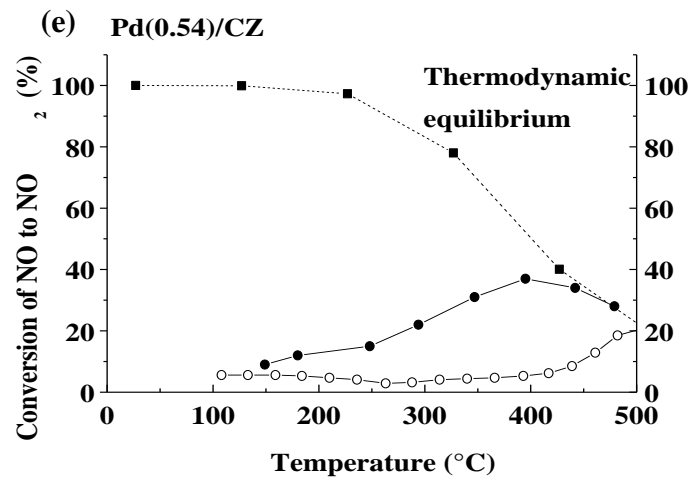
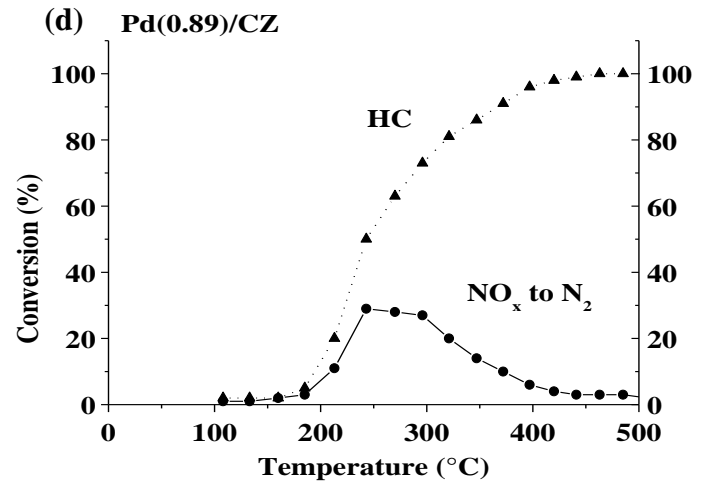
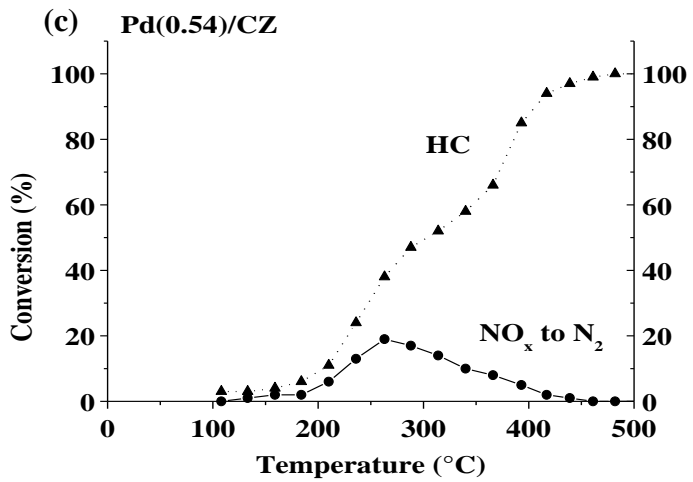
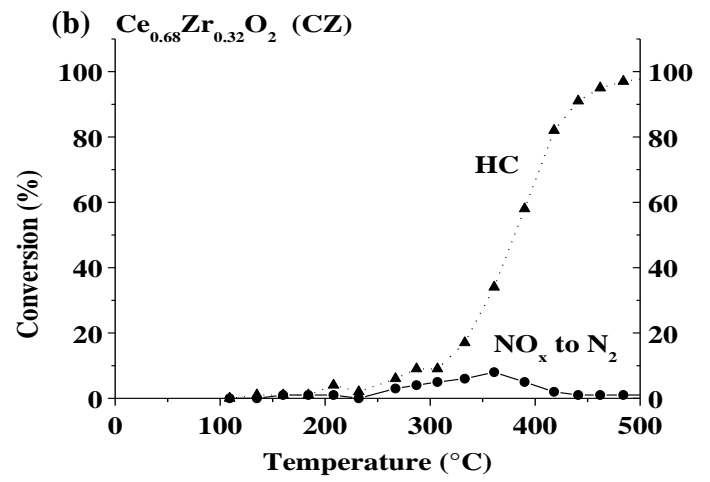
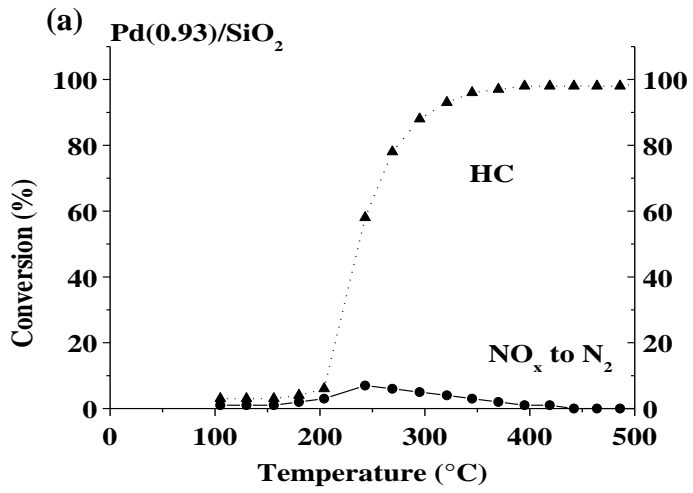


Fig. 10

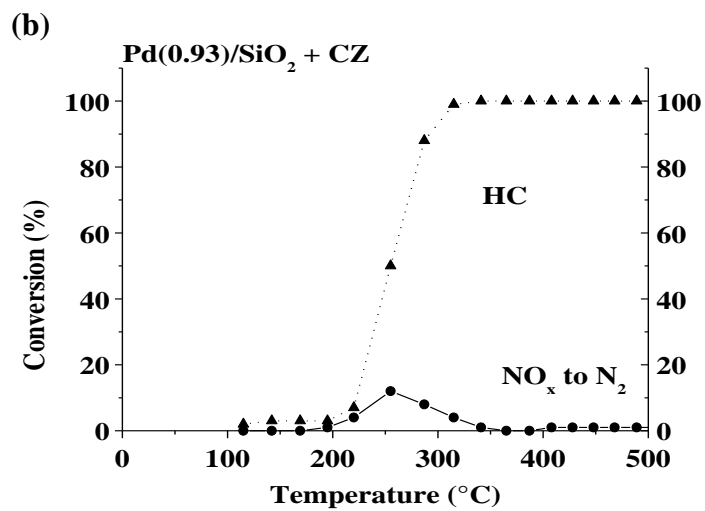
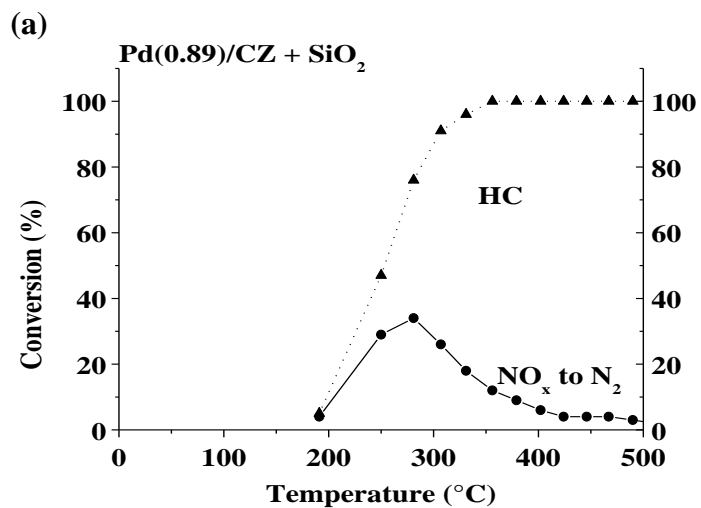


Fig. 11

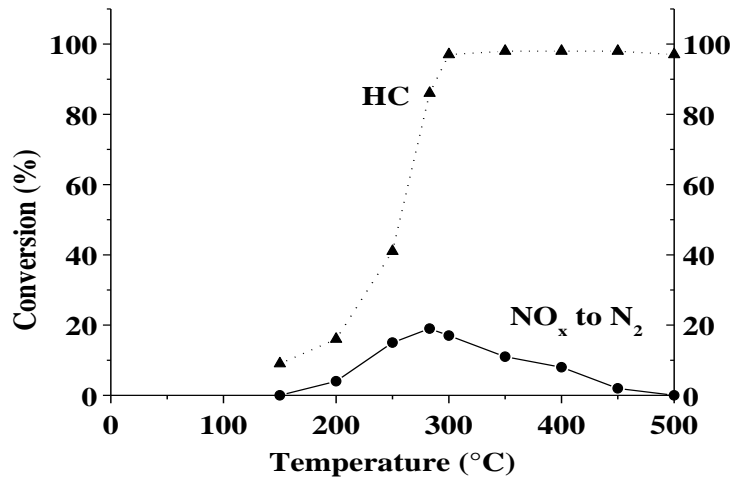


Fig. 12

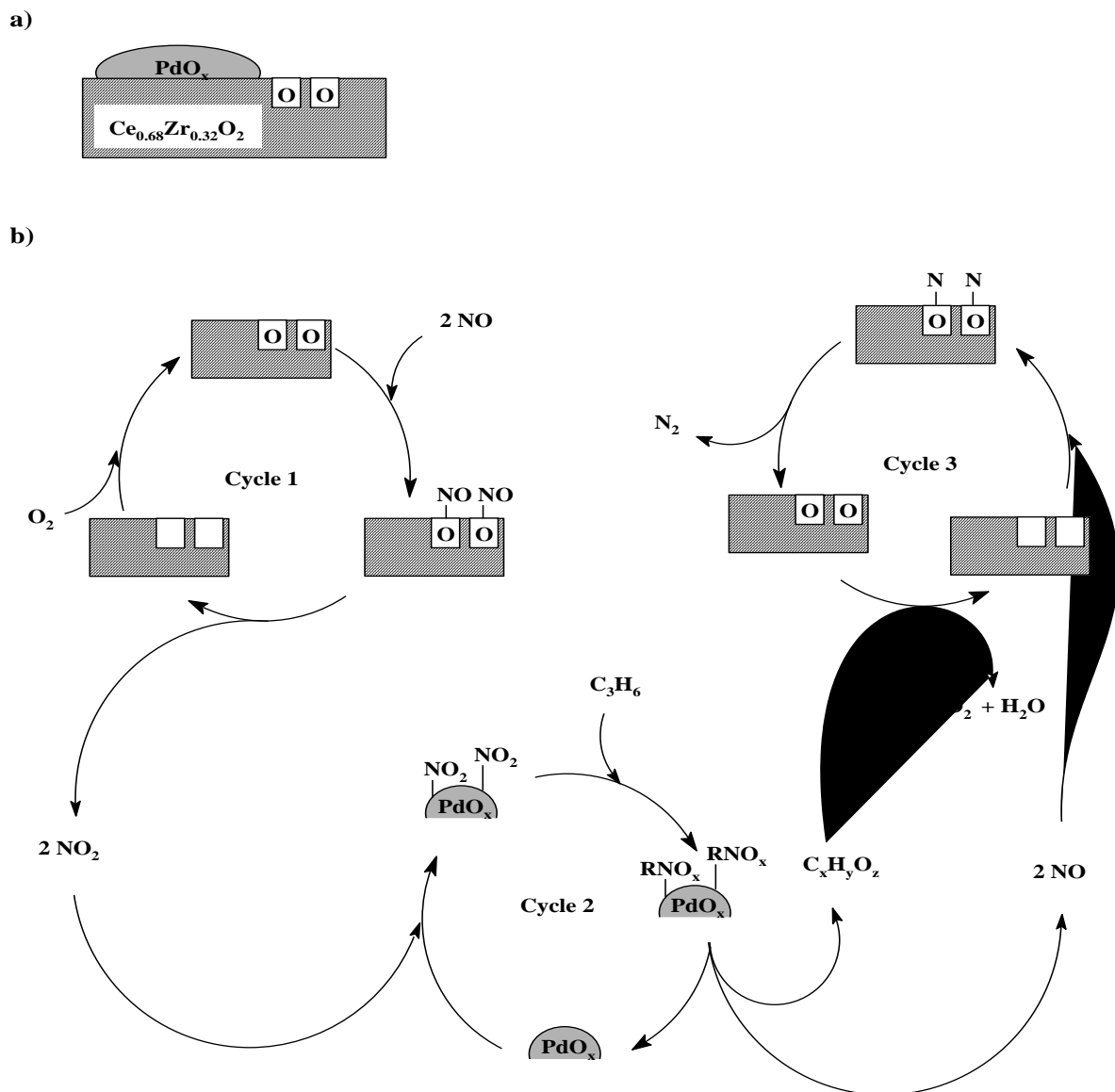


Fig. 13